of the N-terminal half of hCRM1 [amino acids (aa) 1–679) and the C-terminal half of rCRM1 (amino acids (aa) 680–1072), whereas rhCRM1 was its reverse chimera (Fig. 6A). Expression of hrCRM1-HA increased p24 production, whereas there was little enhancement of p24 production by rhCRM1-HA. It should be noted that hCRM1, when expressed at the same level as rCRM1, augmented p24 production but that rCRM1 had no effect, which ruled out the possibility that over-expression of rCRM1 inhibited p24 production. No significant changes in β-gal activity were observed after transfection with CRM1-expressing plasmids (Fig. 6B). These results indicated that the N-terminal region of hCRM1 was involved in the enhanced production of p24.

Discussion

Although initial reports suggested that only fully spliced viral transcripts are detectable and that the effects of Rev are diminished in murine cells (Trono & Baltimore 1990), these findings were not reproduced (Malim & Cullen 1991; Bieniasz & Cullen 2000; Keppler *et al.* 2001). Instead, it was proposed that excessive splicing was responsible for a significant reduction in the levels of viral unspliced RNA species and Gag protein in rodent cells (Zheng *et al.* 2003). Moreover, it has been reported that some rat cells exhibit largely unimpaired expression of Env, a Rev-dependent HIV-1 gene product that is translated from a partially spliced viral mRNA (Keppler *et al.* 2001). One reason for these inconsistent conclusions may have been because of lack to examine the cellular cofactors of Rev, such as CRM1. In both our recent studies and the present study, we found that expression of hCRM1, but not rCRM1, enhanced production of the Gag protein in various rat cells, including macrophages (Okada *et al.* 2009), supporting previous findings of poor Rev activity in these cells.

Although significant export of *gag* mRNA into the cytoplasm of rat cells was observed, we found that hCRM1 enhanced *gag* mRNA export two- to three-fold as indicated by quantitative RT-PCR after cell fractionation and *in situ* hybridization. This increase was in sharp contrast to the 10- to 30-fold augmentation of the Gag protein in the medium. This phenomenon is quite interesting as it has been firmly established that CRM1 is an export factor for Rev, which bridges CRM1 and the viral *gag/env* mRNAs (Cullen 1998, 2003). The aforementioned results suggested that, in addition to simple nucleocytoplasmic transport, CRM1 is somehow involved in regulation of gene expression in the cytoplasm, which affects destination of the cognate protein.

To determine the step during which the activity of hCRM1 differs from that of rCRM1, we examined the stability of the Gag protein using a pulse label and chase experiment. However, the results suggested that hCRM1 does not play a role in prolonging the life of the Gag protein. Neither polyribosome profiling analysis nor the quantification of p55 Gag supported the enhancement of *gag* mRNA translation efficiency by hCRM1. Instead, the data showed that the p55 Gag precursor that was synthesized in the presence of hCRM1, but not rCRM1, underwent efficient processing to the mature Gag protein and budding of virus particles into the culture medium. The results that hCRM1 affects the efficient processing and budding of Gag proteins in rat cells explain the marked enhancement of p24 accumulation in the medium in spite of the minor increase in *gag* mRNA in the cytoplasm in the presence of hCRM1.

Our finding is reminiscent of HIV-1 replication in murine cells where *gag* mRNA, exported through the CTE/Tap pathway, subsequently restored efficient trafficking of the Gag protein to the plasma membrane, thus underlying the efficient processing and budding of HIV Gag, whereas Gag, translated from mRNA exported via the RRE/Rev/CRM1 pathway, was not targeted to the plasma membrane (Swanson *et al.* 2004). The inefficiency of HIV-1 assembly in murine cells likely reflects a cellular deficiency in the RRE/Rev-dependent nuclear export pathway that is specifically linked to the activation of Gag membrane targeting by the regulatory MA globular-head domain (Sherer *et al.* 2009). Similarly, the trafficking of Gag to the plasma membrane was less efficient in rat cells than human cells, which was substantiated by the immunofluorescent localization of p55 Gag protein to the plasma membrane in rat cells, and was not restored by the presence of hCRM1. Thus, hCRM1 may improve budding process but not membrane trafficking of Gag protein in rat cells.

The results suggest that rCRM1 may export *gag* mRNA into the cytoplasm improperly, resulting in the inefficient processing of Gag proteins. It is most likely that CRM1 has an indirect effect on *gag* mRNA in the cytoplasm, because, upon reaching the cytoplasm, it dissociates from the transport complex containing *gag* mRNA, Rev, Ran and other cellular factors via a mechanism in which RanGTP converts to RanGDP at the periphery of the nuclear pore (Fornerod *et al.* 1997; Fukuda *et al.* 1997; Kudo *et al.* 1997; Neville *et al.* 1997; Ossareh-Nazari *et al.* 1997;

Stade *et al.* 1997). Another cellular factor, Rev-interacting protein (hRIP), also known as hRab or Hrb, which is likely bridged by CRM1, has been reported to function in releasing *gag* mRNA, which would otherwise be trapped at the nuclear periphery, to the cytoplasm (Sanchez-Velar *et al.* 2004; Yu *et al.* 2005). Although, in our hands, *in situ* hybridization did not show improper localization of *gag* mRNA in the cytoplasm of rat cells, it is still possible that aberrant construction of the *gag* mRNA transport complex containing rCRM1 might prevent rat Rip and other cellular factors from functional interactions, finally leading to the inefficient processing of Gag proteins.

Alternatively, cytoplasmic effect of hCRM1 could be attributable to the properties of Gag proteins. Gag has capacities for nuclear entry and RNA binding through its NC region, and RNA promotes multimerization of Gag proteins (Muriaux *et al.* 2001; D'Souza & Summers 2005) that may be an important step of viral particle formation. Thus, it is also conceivable that aberrant RNA complex in rat nucleus may cause inefficient Gag multimerization, leading to reduced viral production.

It is possible that hCRM1 may be needed for correct formation of the complex, which can then interact with rat factors and/or Gag proteins appropriately. Our results indicated that hCRM1 exports *gag* mRNA not only more efficiently than rat CRM1 but also correctly, to the cytoplasm in rat cells, leading to the efficient processing of Gag proteins and HIV-1 particle formation. Our finding that HIV-1 production in rat cells was rescued efficiently by the expression of hCRM1 may have important implications for the development of rat animal models of HIV replication and pathogenesis.

Experimental procedures

Cells

Human cell lines, including HeLa, HOS and 293T, and the rat cell lines, ER1/neo1, ER1/hCRM1-7 (Zhang *et al.* 2006), REF52 and W31 (Kanki *et al.* 2000), were maintained in Dulbecco's modified Eagle's medium supplemented with 10% fetal bovine serum in the absence or presence of 300 μg/mL G418 in 10% CO_2 at 37 °C.

Plasmids

The following plasmids were used in this study: pCMVΔR8.2 (Naldini *et al.* 1996); pCRRE (Kimura *et al.* 1996); pSRαhCRM1 and pSRαrCRM1 (Hakata *et al.* 1998, 2001); pSRα296 (Takebe *et al.* 1988); pSRαtat (Takebe *et al.* 1988); pCDMβ-gal (Hakata *et al.* 1998); hCRM1-HA and rCRM1-HA, which carried CRM1, fused at the C terminus to an HA tag (Okada *et al.* 2009); pH1-luc (a kind gift from Dr. A. Adachi), which harbors the luciferase gene downstream of the HIV-1 LTR; and pNLmyr(−)pro(−)Flag and pNLmyr(+)pro(−)Flag (a kind gift from Dr. Y. Morikawa) (Kawada *et al.* 2008).

To construct pSRαhrCRM1-HA and pSRαrhCRM1-HA, the hrCRM1 and rhCRM1 coding regions in pSRαhrCRM1 and pSRαrhCRM1, respectively (Hakata *et al.* 2003), were amplified by PCR using the primer pair for hrCRM1-HA of 5′-GGT CAA TAC CCA CGT TTT TTG AGA GCT CAC TGG A-3′ (the underlined sequence is a *Sac*I site) and 5′-TAT GGT ACC TTA AGC ATA ATC AGG AAC ATC GTA TGG GTA GTC ACA CAT TTC TTC TGG GAT TTC-3′ (the underlined sequence is a *Kpn*I site), and the primer pair for rhCRM1-HA of 5′-CTG GAA TCA CTT GGC AGC TGA GCT CTA CAG AGA GAG TCC A-3′ (the underlined sequence is a *Sac*I site) and 5′-TAT GGT ACC TTA AGC ATA ATC AGG AAC ATC GTA TGG GTA ATC ACA CAT TTC TTC TGG AAT CTC-3′ (the underlined sequence is a *Kpn*I site.), which encodes the HA tag. The PCR was performed using 10 ng of the plasmid as a template, which was denatured at 94 °C for 2 min and was then followed by 20 cycles of amplification: denaturation (94 °C, 30 s), annealing (62 °C, 1 min) and extension (68 °C, 2 min). A final extension was performed at 68 °C for 10 min. The amplified DNA was digested with *Sac*I and *Kpn*I, and inserted into these sites in pSRαhrCRM1 or pSRαrhCRM1, as appropriate.

Real-time RT-PCR

To separate the cytoplasmic and nuclear fractions, lysis buffer (0.5% NP40, 10 mM Tris–HCl [pH 7.4], 0.14 M NaCl, 1.5 mM $MgCl_2$, 1 U/μL RNase Inhibitor (TOYOBO), 1 mM DTT) was added to the cell pellets and the lysates were centrifuged in a microcentrifuge at 500 × *g* for 5 min at 4 °C. Total RNA in the cytoplasm (supernatant) and nucleus (pellet) was extracted using the Absolutely RNA Miniprep Kit (Stratagene). The ThermoScript RT-PCR System (Invitrogen) was used to synthesize cDNAs from 150 to 500 ng of RNA, and the abundance was quantified using real-time PCR with a Light Cycler PCR machine (Roche). PCRs were performed using the following primer pairs: *gag* forward (5′-AGA GAA GGC TTT CAG CCC AGA AGT-3′) and reverse (5′-GGA TTT GTT ACT TGG CTC ATT GCT-3′); *tat* forward (5′-GTG GAA GCA TCC AGG AAG TCA GCC-3′) and reverse (5′-CTA TTC CTT CGG GCC TGT CGG GTC-3′); and *β-gal* forward (5′-GCG AAT ACC TGT TCC G-3′) and reverse (5′-GCG TCA CAC TGA GGT T-3′). PCR mixtures (20 μL) were prepared in a capillary tube containing 1/16 of the volume of the RT reaction mixture, each primer pair (0.5 μM) and 1 × Light Cycler-FastStart SYBR Green PCR Master Mix. After an initial Taq polymerase activation step (95 °C, 15 min), the *gag* and *tat* mRNA amplification reactions were performed using 40 cycles of denaturation (95 °C, 10 s), annealing (68 °C, 10 s) and extension (72 °C, 15 s),

whereas the *β-gal* mRNA was amplified using 40 cycles of denaturation (95 °C, 15 s), annealing (60 °C, 5 s) and extension (72 °C, 11 s). The abundance of each mRNA was estimated with a standard regression curve using the Light Cycler Software v. 3 (Roche). The standard curve was obtained by PCR amplification of 0.0064–500 pg of pCMVΔR8.2 (for *gag* mRNA), pSRαtat and pCDMβ-gal.

To ascertain the efficiency of fractionation, *β-actin* pre-mRNA was amplified by PCR using the primers *β-actin*-F (5′-TCG ATC GCC TTT CTG ACT AGG TG-3′) and *β-actin*-R (5′-GGT CAG GAT CTT CAT GAG GTA GTC TG-3′); the former targets the intron and the latter targets the exon of *β-actin* pre-mRNA. Reactions were performed with 25 cycles of denaturation at 94 °C for 30 s, followed by annealing at 59 °C for 1 min and extension at 72 °C for 30 s.

Pulse chase assay

At 36 to 48 h post-transfection, cells were metabolically labeled with an [^{35}S]-methionine/cysteine mixture (GE Healthcare UK Ltd.) for 30 min. Cells were washed once and then chased for 0, 4, 8 and 24 h in 1 mL of medium supplemented with 10 μM methionine, 10 μM cysteine and 100 nM KNI-272 (an HIV-1 protease inhibitor, the kind gift of Dr. Y. Kiso). After chasing, 0.25 mL of 5× detergent buffer containing 2.5% deoxycholate, 2.5% Triton ×100, 250 mM Tris–HCl (pH 7.6), 0.1 M NaCl, 0.1 M EDTA, 100 nM KNI-272 and a protease inhibitor cocktail (Roche) was added to the culture to dissolve Gag proteins in both the medium and cells. The lysates were centrifuged in a microcentrifuge at 7200 × *g* for 15 min, and the supernatant was incubated with anti-Gag mAb V107 (Ikuta *et al.* 1989) (a kind gift from Dr. K. Ikuta) for 1 h at 4 °C, followed by incubation with protein-G Sepharose for 1 h at 4 °C. After three washes with detergent buffer, the precipitated complexes were analyzed by SDS–PAGE and autoradiography.

At 40 h post-transfection with pNLmyr(−)pro(−)Flag, cells were metabolically labeled with an [^{35}S]-methionine/cysteine mixture for 15 min, washed and then chased for 0, 4 and 7 h as described earlier. The detergent buffer (0.5 mL) was added to the cells and centrifuged in a microcentrifuge at 7200 × *g* for 15 min. The supernatant was incubated with anti-Flag M2 antibody (Sigma) conjugated to protein-G Sepharose for 3 h at 4 °C, followed by three washes with the detergent buffer.

In situ hybridization

At 48 to 50 h after transfection, cells were subjected to an *in situ* hybridization assay, which has been described previously (Tautz & Pfeifle 1989; Kimura *et al.* 1996). Probes were prepared by PCR amplification of a 167-bp fragment from HIV-1 *gag* using the primers T66 (5′-GAGAGCGTCGGT ATTAAG-3′; HIV-1_{NL4-3} nts 798–815) and T67 (5′-GTC TACAGCCTTCTGATG-3′; HIV-1 $_{NL4-3}$ nts 964–947). The fragment generated was then used as a template for a second PCR, using either T67 or T66 primers and the digoxigenin (DIG)-nucleotide mixture (Roche), essentially as described by Tautz & Pfeifle (1989). Cells were examined under a confocal laser-scanning microscope (Olympus).

Western blotting

The transfected cells were dissolved in TMN buffer containing 10 mM Tris–HCl (pH 7.4), 2 mM $MgCl_2$, 0.5% NP40 and a protease inhibitor cocktail. After measuring the β-gal activity and protein levels, the proteins were solubilized with sample buffer and resolved by SDS–PAGE and then transferred to a nitrocellulose filter. V107, a rat anti-HA mAb (Roche), a rabbit anti-β-gal Ab, a mouse anti-actin mAb and anti-FLAG M2 Ab were used as primary Abs. Horseradish peroxidase-conjugated anti-IgG Abs (Promega) were used as secondary Abs. Immunoreactive bands were visualized using ECL + plus (GE Health care) followed by the LAS-1000 Plus system (Fujifilm) and were evaluated by Image Gauge (version 3.4) software (Fujifilm).

Immunofluorescence

Subconfluent ER1/neo1 cells, seeded onto coverslips (Fisher Scientific) in six-well plates, were transfected using Polyethylenimine 'Max' (PEI) (Polyscience) and fixed 18 h post-transfection with 2% paraformaldehyde dissolved in PBS. The cells were then permeabilized with 0.5% NP40 in PBS and incubated with blocking solution (5% skim milk in PBS) for 1 h at RT. The cells were stained with Alexa Fluor488-conjugated anti-HA-Tag (6E2) mouse mAb and Alexa Fluor® 555-conjugated anti-DYKDDDDK (FLAG) Tag antibody (Cell Signaling Technology) for 1 h at RT, washed and then mounted with VECTASHIELD Hard set Mounting Medium (Vector Laboratories). The stained cells were examined under a confocal laser-scanning microscope.

Preparation of VLP

To prepare the viral-like particle (VLP) fraction, medium from the cell cultures was centrifuged at 530 × *g* for 10 min and the supernatant was filtered through a Millex HV 0.45 μm Filter Unit (Millipore). The HIV-1 particles were pelleted through a 20% (W/V) sucrose solution by centrifugation at 86,000 × *g* in an SW28 rotor for 2 h at 4 °C.

Statistical analysis

Comparisons between individual data points were made using a Student's *t*-test. Two-sided *P*-values ≤ 0.05 were considered statistically significant.

Acknowledgements

We thank Dr J. Fujisawa for kind administration, and K. Ofuji, A. Hirano, N. Mizuno and S. Yamanouchi for excellent technical assistance. V107, pH1-luc, pNLmyr(−)pro(−)Flag, and KNI-272 were kind gifts from Dr K. Ikuta (University of

Osaka), Dr A. Adachi (Tokushima University), Dr Y. Morikawa (Kitazato University) and Dr Y. Kiso (Kyoto Pharmaceutical University), respectively. This study was supported by grants from the Ministry of Sports and Culture (Japan) and the Ministry of Health and Welfare (Japan).

References

Bieniasz, P.D. & Cullen, B.R. (2000) Multiple blocks to human immunodeficiency virus type 1 replication in rodent cells. *J. Virol.* **74**, 9868–9877.

Browning, J., Horner, J.W., Pettoello-Mantovani, M., Raker, C., Yurasov, S., DePinho, R.A. & Goldstein, H. (1997) Mice transgenic for human CD4 and CCR5 are susceptible to HIV infection. *Proc. Natl Acad. Sci. USA* **94**, 14637–14641.

Cullen, B.R. (1998) Retroviruses as model systems for the study of nuclear RNA export pathways. *Virology* **249**, 203–210.

Cullen, B.R. (2003) Nuclear RNA export. *J. Cell Sci.* **116**, 587–597.

D'Souza, V. & Summers, M.F. (2005) How retroviruses select their genomes. *Nat. Rev. Microbiol.* **3**, 643–655.

Fornerod, M., Ohno, M., Yoshida, M. & Mattaj, I.W. (1997) CRM1 is an export receptor for leucine-rich nuclear export signals. *Cell* **90**, 1051–1060.

Fukuda, M., Asano, S., Nakamura, T., Adachi, M., Yoshida, M., Yanagida, M. & Nishida, E. (1997) CRM1 is responsible for intracellular transport mediated by the nuclear export signal. *Nature* **390**, 308–311.

Giuffre, A.C., Higgins, J., Buckheit, R.W. Jr & North, T.W. (2003) Susceptibilities of simian immunodeficiency virus to protease inhibitors. *Antimicrob. Agents Chemother.* **47**, 1756–1759.

Goffinet, C., Michel, N., Allespach, I., Tervo, H.M., Hermann, V., Krausslich, H.G., Greene, W.C. & Keppler, O.T. (2007) Primary T-cells from human CD4/CCR5-transgenic rats support all early steps of HIV-1 replication including integration, but display impaired viral gene expression. *Retrovirology* **4**, 53.

Hakata, Y., Umemoto, T., Matsushita, S. & Shida, H. (1998) Involvement of human CRM1 (exportin 1) in the export and multimerization of the Rex protein of human T-cell leukemia virus type 1. *J. Virol.* **72**, 6602–6607.

Hakata, Y., Yamada, M., Mabuchi, N. & Shida, H. (2002) The carboxy-terminal region of the human immunodeficiency virus type 1 protein Rev has multiple roles in mediating CRM1-related Rev functions. *J. Virol.* **76**, 8079–8089.

Hakata, Y., Yamada, M. & Shida, H. (2001) Rat CRM1 is responsible for the poor activity of human T-cell leukemia virus type 1 Rex protein in rat cells. *J. Virol.* **75**, 11515–11525.

Hakata, Y., Yamada, M. & Shida, H. (2003) A multifunctional domain in human CRM1 (exportin 1) mediates RanBP3 binding and multimerization of human T-cell leukemia virus type 1 Rex protein. *Mol. Cell. Biol.* **23**, 8751–8761.

Hazuda, D.J., Young, S.D., Guare, J.P., *et al.* (2004) Integrase inhibitors and cellular immunity suppress retroviral replication in rhesus macaques. *Science* **305**, 528–532.

Hu, S.L. (2005) Non-human primate models for AIDS vaccine research. *Curr. Drug Targets Infect. Disord.* **5**, 193–201.

Ikuta, K., Morita, C., Miyake, S., Ito, T., Okabayashi, M., Sano, K., Nakai, M., Hirai, K. & Kato, S. (1989) Expression of human immunodeficiency virus type 1 (HIV-1) gag antigens on the surface of a cell line persistently infected with HIV-1 that highly expresses HIV-1 antigens. *Virology* **170**, 408–417.

Kanki, K., Torigoe, T., Hirai, I., Sahara, H., Kamiguchi, K., Tamura, Y., Yagihashi, A. & Sato, N. (2000) Molecular cloning of rat NK target structure–the possibility of CD44 involvement in NK cell-mediated lysis. *Microbiol. Immunol.* **44**, 1051–1061.

Kawada, S., Goto, T., Haraguchi, H., Ono, A. & Morikawa, Y. (2008) Dominant negative inhibition of human immunodeficiency virus particle production by the nonmyristoylated form of gag. *J. Virol.* **82**, 4384–4399.

Keppler, O.T., Welte, F.J., Ngo, T.A., *et al.* (2002) Progress toward a human CD4/CCR5 transgenic rat model for de novo infection by human immunodeficiency virus type 1. *J. Exp. Med.* **195**, 719–736.

Keppler, O.T., Yonemoto, W., Welte, F.J., Patton, K.S., Iacovides, D., Atchison, R.E., Ngo, T., Hirschberg, D.L., Speck, R.F. & Goldsmith, M.A. (2001) Susceptibility of rat-derived cells to replication by human immunodeficiency virus type 1. *J. Virol.* **5**, 8063–8073.

Kimura, T., Hashimoto, I., Nishikawa, M. & Fujisawa, J.I. (1996) A role for Rev in the association of HIV-1 gag mRNA with cytoskeletal beta-actin and viral protein expression. *Biochimie* **78**, 1075–1080.

Kudo, N., Khochbin, S., Nishi, K., Kitano, K., Yanagida, M., Yoshida, M. & Horinouchi, S. (1997) Molecular cloning and cell cycle-dependent expression of mammalian CRM1, a protein involved in nuclear export of proteins. *J. Biol. Chem.* **272**, 29742–29751.

Malim, M.H. & Cullen, B.R. (1991) HIV-1 structural gene expression requires the binding of multiple Rev monomers to the viral RRE: implications for HIV-1 latency. *Cell* **65**, 241–248.

Malim, M.H., McCarn, D.F., Tiley, L.S. & Cullen, B.R. (1991) Mutational definition of the human immunodeficiency virus type 1 Rev activation domain. *J. Virol.* **65**, 4248–4254.

Marques, S.M., Veyrune, J.L., Shukla, R.R. & Kumar, A. (2003) Restriction of human immunodeficiency virus type 1 Rev function in murine A9 cells involves the Rev C-terminal domain. *J. Virol.* **77**, 3084–3090.

Muriaux, D., Mirro, J., Harvin, D. & Rein, A. (2001) RNA is a structural element in retrovirus particles. *Proc. Natl Acad. Sci. USA* **98**, 5246–5251.

Nakielny, S. & Dreyfuss, G. (1999) Transport of proteins and RNAs in and out of the nucleus. *Cell* **99**, 677–690.

Naldini, L., Blomer, U., Gallay, P., Ory, D., Mulligan, R., Gage, F.H., Verma, I.M. & Trono, D. (1996) *In vivo* gene

delivery and stable transduction of nondividing cells by a lentiviral vector. *Science* **272**, 263–267.

Neville, M., Stutz, F., Lee, L., Davis, L.I. & Rosbash, M. (1997) The importin-beta family member Crm1p bridges the interaction between Rev and the nuclear pore complex during nuclear export. *Curr. Biol.* **7**, 767–775.

Okada, H., Zhang, X., Fofana, I.B., Nagai, M., Suzuki, H., Ohashi, T. & Shida, H. (2009) Synergistic effect of human CycT1 and CRM1 on HIV-1 propagation in rat T cells and macrophages. *Retrovirology* **6**, 43.

Ossareh-Nazari, B., Bachelerie, F. & Dargemont, C. (1997) Evidence for a role of CRM1 in signal-mediated nuclear protein export. *Science* **278**, 141–144.

Sanchez-Velar, N., Udofia, E.B., Yu, Z. & Zapp, M.L. (2004) hRIP, a cellular cofactor for Rev function, promotes release of HIV RNAs from the perinuclear region. *Genes Dev.* **18**, 23–34.

Sherer, N.M., Swanson, C.M., Papaioannou, S. & Malim, M.H. (2009) Matrix mediates the functional link between human immunodeficiency virus type 1 RNA nuclear export elements and the assembly competency of Gag in murine cells. *J. Virol.* **83**, 8525–8535.

Shultz, L.D., Ishikawa, F. & Greiner, D.L. (2007) Humanized mice in translational biomedical research. *Nat. Rev. Immunol.* **7**, 118–130.

Stade, K., Ford, C.S., Guthrie, C. & Weis, K. (1997) Exportin 1 (Crm1p) is an essential nuclear export factor. *Cell* **90**, 1041–1050.

Swanson, C.M., Puffer, B.A., Ahmad, K.M., Doms, R.W. & Malim, M.H. (2004) Retroviral mRNA nuclear export elements regulate protein function and virion assembly. *The EMBO J.* **23**, 2632–2640.

Takayanagi, R., Ohashi, T., Yamashita, E., Kurosaki, Y., Tanaka, K., Hakata, Y., Komoda, Y., Ikeda, S., Tsunetsugu-Yokota, Y., Tanaka, Y. & Shida, H. (2007) Enhanced replication of human T-cell leukemia virus type 1 in T cells from transgenic rats expressing human CRM1 that is regulated in a natural manner. *J. Virol.* **81**, 5908–5918.

Takebe, Y., Seiki, M., Fujisawa, J., Hoy, P., Yokota, K., Arai, K., Yoshida, M. & Arai, N. (1988) SR alpha promoter: an efficient and versatile mammalian cDNA expression system composed of the simian virus 40 early promoter and the R-U5 segment of human T-cell leukemia virus type 1 long terminal repeat. *Mol. Cell. Biol.* **8**, 466–472.

Tautz, D. & Pfeifle, C. (1989) A non-radioactive *in situ* hybridization method for the localization of specific RNAs in Drosophila embryos reveals translational control of the segmentation gene hunchback. *Chromosoma* **98**, 81–85.

Trono, D. & Baltimore, D. (1990) A human cell factor is essential for HIV-1 Rev action. *EMBO J.* **9**, 4155–4160.

Veazey, R.S., Klasse, P.J., Schader, S.M., Hu, Q., Ketas, T.J., Lu, M., Marx, P.A., Dufour, J., Colonno, R.J., Shattock, R.J., Springer, M.S. & Moore, J.P. (2005) Protection of macaques from vaginal SHIV challenge by vaginally delivered inhibitors of virus-cell fusion. *Nature* **438**, 99–102.

Watanabe, S., Terashima, K., Ohta, S., Horibata, S., Yajima, M., Shiozawa, Y., Dewan, M.Z., Yu, Z., Ito, M., Morio, T., Shimizu, N., Honda, M. & Yamamoto, N. (2007) Hematopoietic stem cell-engrafted NOD/SCID/IL2R-gamma null mice develop human lymphoid systems and induce long-lasting HIV-1 infection with specific humoral immune responses. *Blood* **109**, 212–218.

Yu, Z., Sanchez-Velar, N., Catrina, I.E., Kittler, E.L., Udofia, E.B. & Zapp, M.L. (2005) The cellular HIV-1 Rev cofactor hRIP is required for viral replication. *Proc. Natl Acad. Sci. USA* **102**, 4027–4032.

Zhang, X., Hakata, Y., Tanaka, Y. & Shida, H. (2006) CRM1, an RNA transporter, is a major species-specific restriction factor of human T cell leukemia virus type 1 (HTLV-1) in rat cells. *Microbes Infect.* **8**, 851–859.

Zheng, Y.H., Yu, H.F. & Peterlin, B.M. (2003) Human p32 protein relieves a post-transcriptional block to HIV replication in murine cells. *Nat. Cell Biol.* **5**, 611–618.

Received: 2 October 2010
Accepted: 1 November 2010

Supporting Information/Supplementary material

The following Supporting Information can be found in the online version of the article:

Figure S1 Polyribosome profile analysis of *gag*, *tat* and *b-gal* mRNAs in the presence or absence of hCRM1.

Data S1 Materials and method.

Additional Supporting Information may be found in the online version of this article.

Please note: Wiley-Blackwell are not responsible for the content or functionality of any supporting materials supplied by the authors. Any queries (other than missing material) should be directed to the corresponding author for the article.

Regulation of the susceptibility of HIV-1 to a neutralizing antibody KD-247 by nonepitope mutations distant from its epitope

Mari Takizawa[a], Kosuke Miyauchi[a], Emiko Urano[a], Shigeru Kusagawa[a], Katsuhiko Kitamura[b], Satoshi Naganawa[c], Toshio Murakami[d], Mitsuo Honda[e], Naoki Yamamoto[f] and Jun Komano[a]

Objective: A humanized neutralizing antibody, KD-247, targets the V3 loop of HIV-1 Env. HIV-1 bearing the GPGR sequence at the V3 loop is potentially susceptible to KD-247. However, not all GPGR-positive HIV-1 isolates are neutralized by KD-247. We examined the potential mechanism by which the susceptibility of HIV-1 to KD-247-mediated neutralization is regulated.

Design: We searched for nonepitope neutralization regulatory (NNR) mutations that sensitize GPGR-bearing HIV-1_{AD8} to KD-247 and mapped the locations of such mutations relative to the V3 loop.

Methods: We generated a functional HIV-1_{AD8} Env library, and evaluated the viral susceptibility to KD-247 by measuring the half-inhibitory concentration (IC_{50}) to KD-247 on TZM-bl cell assay.

Results: We identified nine KD-247-sensitizing NNR mutations from 30 mutations in various regions of gp120, including the V1/V2 loop, C2, V3 loop, C4, and C5. They specifically affected KD-247-mediated neutralization, as they did not affect the b12-mediated neutralization. When combined, the KD-247-sensitizing NNR mutations additively sensitized the virus to KD-247 by up to 10 000 folds. The KD-247-sensitizing NNR mutations increased KD-247 binding to the virion. Notably, the NNR mutation in C4 coincides with the CD4-binding site of gp120.

Conclusion: Given that most of the KD-247-sensitizing NNR mutations are remote from V3 loop, it is reasonable to hypothesize that the steady-state, local conformation of the V3 loop is regulated by the interdomain contact of gp120. Our mutational analysis complements crystallographic studies by helping provide a better understanding of the steady-state conformation and the functional geometry of Env.

AIDS 2011, **25**:2209–2216

Keywords: envelope, HIV-1, KD-247, neutralization, steady-state conformation

Introduction

HIV-1 is a highly mutagenic virus. The viral envelope glycoprotein gp120/41 (Env) accumulates mutations to escape from the host humoral immunity. The study on HIV-1-neutralizing antibodies (Nabs) and the viral escape from Nab gives us insights into viral pathogenesis, structure–function relationship of Env, and AIDS vaccine design [1–8].

[a]AIDS Research Center, National Institute of Infectious Diseases, Tokyo, [b]Department of Public Health, Yokohama City University School of Medicine, Yokohama, [c]Infectious Disease Regulation Project, The Tokyo Metropolitan Institute of Medical Science, Tokyo, [d]The Chemo-Sero-Therapeutic Research Institute, Kumamoto, [e]Department of Pathology and Microbiology, Division of Microbiology, Nihon University School of Medicine, Tokyo, Japan, and [f]Department of Microbiology, Yong Loo Lin School of Medicine, National University of Singapore, Singapore.

Correspondence to Jun Komano, AIDS Research Center, National Institute of Infectious Diseases, 1-23-1 Toyama Shinjuku, Tokyo 162-8640, Japan.

Tel: +81 3 5285 1111; fax: +81 3 5285 5037; e-mail: ajkomano@nih.go.jp
Received: 8 September 2010; revised: 4 July 2011; accepted: 5 August 2011.

DOI:10.1097/QAD.0b013e32834bab68

ISSN 0269-9370 © 2011 Wolters Kluwer Health | Lippincott Williams & Wilkins

A humanized monoclonal Nab, KD-247, which is effective against half of clade B primary HIV-1 isolates, targets the third hypervariable (V3) loop, is an attractive AIDS vaccine target [1–3]. The epitope essential for KD-247-mediated neutralization is the conserved tetrapeptide sequence GPGR (HXB2 coordinate 312–315). A human monoclonal Nab 447–52D targets this same epitope [4]. Mutations in the GPGR sequence confer viral resistance to KD-247 [3,5,6]. Moreover, amino acid changes adjacent to the GPGR motif have also conferred viral resistance to KD-247 (e.g. H, R, and K at 311 position, or P at 316 position) [3]. Such mutations physically interfere with binding to the KD-247 epitope [3]. In the absence of such mutations, HIV-1 bearing the GPGR sequence at the V3 loop is potentially susceptible to KD-247. However, not all GPGR-positive HIV-1 isolates are neutralized by KD-247. The mechanism by which some of the GPGR-bearing viruses are resistant to KD-247 is not fully understood.

We addressed this sequence-neutralization susceptibility discordance by comparing the amino acid sequences of various HIV-1 primary isolates. We defined a virus as resistant to KD-247-mediated neutralization when the half-inhibitory concentration (IC_{50}) was higher than 100 μg/ml. We analyzed V3 loop amino acid sequences from 25 viruses positive for the GPGR epitope, including 11 KD-247-sensitive and 14 KD-247-resistant viruses. Along with the ELISA data in our previous report [3], we found that H304R contributes to KD-247 resistance. The H304R polymorphism accounted for 35.7% (five of 14 isolates) of the examples of sequence-neutralization susceptibility discordance, but all the viruses carrying H304R were CRF01_AE. We failed to identify any neutalization regulatory mutations in the clade B isolates. Additionally, the KD-247 prototype mouse monoclonal antibody C25 was unable to neutralize 17 GPGR-positive HIV-1 clade B primary isolates, even though C25 was able to bind their synthetic V3 loop peptides (unpublished observation). From these data, we postulated that the sequence-neutralization susceptibility discordance is due to non-epitope neutralization regulatory (NNR) mutations, especially remote from the V3 loop. Such NNR mutations would be positioned at certain key sites within the Env domains and regulate the steady-state conformation. NNR mutations have been predicted for 447–52D and other cross-reactive Nab [6–11]. To test this hypothesis, we examined 15 entire Env amino acid sequences of KD-247-sensitive and KD-247-resistant viruses. However, we were unable to identify amino acids associated with susceptibility to KD-247. This suggests that the heterologous virus approach is not sensitive enough to identify NNR mutations because the diversity of Env amino acid sequences is beyond the level of detection.

Here we employed a genetic approach to identify NNR mutations using the HIV-$1_{AD8/ADA}$ (AD8 hereafter), which displays the sequence-neutralization susceptibility discordance. The AD8 strain has been reported to be sensitive to 447–52D, which targets the same neutralization epitope as KD-247 within the V3 loop [10], suggesting that the GPGR epitope of the V3 loop is open to antibodies. We thought that this should help understand how the NNR mutations work. It does not contain insertions adjacent to the GPGR motif, as HIV-1_{HXB2} or HIV-1_{NL4-3} do (QR insertion before I and G) nor H304R. Only a few NNR mutations that make HIV-1 resistant to KD-247 have been reported in the V1/V2 loop [6]. In this work, we generated a functional AD8 Env library to identify many NNR mutations simultaneously that cause HIV-1 to become susceptible to KD-247. Through KD-247-sensitizing NNR mutations, we tried to understand the regulatory mechanism of the viral susceptibility to KD-247-mediated neutralization.

Materials and methods

Cells, viruses, and transfection

Cells were maintained in RPMI-1640 Medium (Sigma, St Louis, Missouri, USA) supplemented with 10% fetal bovine serum (FBS) (Japan Bioserum, Tokyo, Japan), 50 U/ml penicillin, and 50 μg/ml streptomycin (Invitrogen, Tokyo, Japan), at 37°C in a humidified 5% CO_2 atmosphere. Cells were transfected with Lipofectamine 2000 according to the manufacturer's protocol (Invitrogen). The other viruses and TZM-bl cells were obtained from the NIH AIDS Research and Reference Reagent Program.

Antibodies

KD-247 was provided by the Chemo-Sero-Therapeutic Research Institute, and b12 is a generous gift from Dr Burton (The Scripps Research Institute).

Cloning

AD8 Env was amplified by nested reverse-transcriptase-PCR using RNA extracted from the culture supernatant as a template (RNeasy mini kit; Qiagen, Hilden, Germany). The primers used were as follows. For the first PCR, the sense primer was 5′-ATG AAA CTT ACG GGG ATA CTT GGG-3′ (HXB2 nucleotide coordinates 5698–5721) and the antisense primer was 5′-GGT ACT AGC TTG AAG CAC CAT CC-3′ (HXB2 nucleotide coordinates 9236–9214); and for the nested PCR, the sense primer was 5′-ATA AGA ATT CTG CAA CAA CTG CTG-3′ (HXB2 nucleotide coordinates 5739–5762) and the antisense primer was 5′-TTC CAG GTC TCG AGA TGC TGC-3′ (HXB2 nucleotide coordinates 8910–8890). EcoRI-XhoI fragments of the PCR products were cloned into the corresponding restriction sites of pNL4–3. The *env* gene was sequenced using the following primers: 3479a, 5′-CTT GGG ATG TTG

ATG ATC TGT AGT GCT GTA GA-3′; 003A, 5′-AGC AGA AGA CAG TGG CAA TG-3′; 106A, 5′-CAT ACA TTA TTG TGC CCC GGC TGG-3′; 545A, 5′-GAC AAT TGG AGA AGT GAA TT-3′; and 5700, 5′-AGC CTG TGC CTC TTC AGC TAC CAC CGC TTG-3′.

Neutralization assay

To produce virus from proviral DNA, 293FT cells (Cat# R700–007; Invitrogen) grown in six-well plates were transfected with proviral DNA-encoding plasmid (1 μg) using Lipofectamine 2000, and replated into a six-well plate at 4–6 h posttransfection. At 48 h posttransfection, the cell culture medium was collected and mixed with dextran (final concentration 16.25 μg/ml, DEAE-Dextran chloride, molecular weight ~500 kDa; ICN Biomedicals Inc., Aurora, Ohio, USA). The TZM-bl cells were plated in 96-well plates at 500 cells per well in a volume of 100 μl a day before infection. The virus and KD-247 were mixed in a volume of 50 μl and incubated at 37°C for 30 min. Then, the TZM-bl cells were exposed to the virus-KD-247 mixture. At 3 days postinfection, luciferase activity was measured using the Steady-Glo Luciferase Assay system (Promega, Madison, Wisconsin, USA). The IC_{50} was defined as the Nab concentration that yielded a half-reduction in luciferase activity compared with the control wells after subtracting background signals as previously described [12]. Luminescence was detected using a Veritas Microplate Luminometer (Promega). The GHOST cell-based and peripheral blood mononuclear cell-based neutralization assays were performed as described previously [3].

Virus capture ELISA

The ELISA plate (Nunclon, Roskilde, Denmark) was coated by KD-247 with incubating plates with 100 μl of KD-247 preparation (10 μg/ml) in a carbonate buffer (15 mmol/l Na_2CO_3, 35 mmol/l $NaHCO_3$, pH 9.6) at 4°C overnight. Plates were washed five times with Plate Wash Buffer (Zeptometrics, Buffalo, New York, USA), and blocked with PBS containing 20% FBS (Nalgene, Rochester, New York) at 37°C for 1 h. After washing the plates for five times with Plate Wash Buffer and once with PBS, virus was captured by KD-247 by incubating plates with viral preparations containing 50 ng of $p24^{CA}$ resuspended in a volume of 100 μl PBS. After washing PBS with 10% FBS, captured virus was lysed in a buffer and a $p24^{CA}$ ELISA was conducted according to the manufacturer's protocol (Zeptometrics).

Results

Construction of a functional Env library based on the AD8 strain

In theory, it is possible to identify NNR mutations conferring viral resistance to the Nab by selecting Nab-resistant mutants from a Nab-sensitive virus in culture. However, this approach is not ideal for the identification of many NNR mutations at the same time because it primarily selects epitope mutants and only a few dominant NNR mutants. To overcome this problem, we tried to identify NNR mutations that sensitize HIV-1 to KD-247. To achieve this goal, we generated a functional Env library and tried to identify KD-247-sensitizing NNR mutations by correlating mutations with viral susceptibility to KD-247-mediated neutralization. We chose a KD-247-resistant strain, AD8, that shows sequence-neutralization susceptibility discordance, and its IC_{50} to KD-247, when the virus is produced in 293T cells from a proviral DNA, was 354.9 μg/ml by TZM-bl assay (average of five independent experiments). Interestingly, this strain has been reported to be sensitive to 447–52D, which targets the same neutralization epitope within the V3 loop [10]. This suggests that the GPGR epitope of the V3 loop is open to antibodies, and the hindrance of KD-247 epitope is unlikely.

An Env mutant library can be produced by genetic engineering (e.g., PCR-based random mutagenesis). However, such an approach does not always produce functional Env. In contrast, Env mutants generated by viral diversification in tissue culture should be functional unless sporadic mutations that interfere with Env function are introduced. We took the latter approach to generate a functional Env library. We diversified AD8 viruses by approximately 100 passages in MOLT-4 cells. This was a simple bulk passage of virus, whereby tissue culture supernatant was transferred to fresh cells, likely conferring the survival of random mutations. We examined the diversity by sequencing 56 *env* clones. Of these 56 clones, 54 *env* clones were independent, suggesting that the diversification of *env* was successful. The IC_{50} of diversified AD8 to KD-247 was 334.6 μg/ml by TZM-bl assay (average of three independent experiments), suggesting that the diversified AD8 is resistant to KD-247 when scored in bulk. Our data indicate that long-term viral selection in tissue culture does not necessarily select a few dominant mutants; various mutants of independent origins can be maintained. We expected that most of the amino acid substitution mutations should not damage Env function; otherwise, they should not have been selected in culture. The average number of mutations was 3.0 per clone, including the frameshift and stop codon mutations, and, importantly, every virus retained the GPGR epitope in the V3 loop. These viruses were distinct from each other but not as divergent as a panel of field isolates, making them suitable for the identification of KD-247-sensitizing NNR mutations. Our diversification protocol does not necessarily select Env mutants with higher or lower susceptibility to KD-247. We expect that some (but not all) mutations may increase the susceptibility to KD-247. We next evaluated whether any mutations could confer the increased susceptibility of the AD8 strain to KD-247.

Identification of nonepitope neutralization regulatory mutations in various domains of gp120

In our viral diversification protocol, mutations can occur in any region of the viral genome. We are concerned that non-Env mutations could affect neutralization susceptibility to KD-247. For example, the IC_{50} could be scored lower if the viral fitness is poor and higher if viral fitness is high. To avoid these possibilities, we cloned diversified Env into the same viral genetic background. We chose HIV-1_{NL4-3} because it is one of the standard molecular clones of HIV-1, and the proviral DNA is relatively stable and, thus, suitable for such cloning. The AD8 *env* cloned HIV-1_{NL4-3} was named NL/AD8. At first, we verified that the susceptibility of viral isolates to KD-247-mediated neutralization could be reproduced on the HIV-1_{NL4-3} genetic background. For this purpose, we used HIV-1_{MN} and AD8 Env, which are highly susceptible and resistant to KD-247, respectively. Cloning *env* from KD-247-sensitive HIV-1_{MN} into HIV-1_{NL4-3} reproduced neutralization susceptibility (IC_{50} 0.07 μg/ml). Similarly, the KD-247 resistance seen in the AD8 strain was reproduced in the NL/AD8 viruses (IC_{50} 357.5 μg/ml, Table 1). Env mutants with no stop codon or frameshift were tested on the HIV-1_{NL4-3} background. Chimeric viruses carrying AD8 Env mutants that did not yield and infectivity index in TZM-bl cells comparable to that of viruses carrying NL4–3/AD8 were not tested further. Viruses bearing combinations of mutations were generated by positioning mutations between useful restriction enzyme recognition sites in the viral genome. Finally, we examined 27 molecular clones by substituting HIV-1_{NL4-3} *env* with the diversified AD8 *env* clones or AD8 *env* with a point mutation found in the diversified pool (Table 1) Mutations causing Env amino acid changes did not comutate the viral proteins encoded in the Env-overlapping frames including *vpu, tat*, and *rev*.

We determined the IC_{50} of KD-247 on these viruses using TZM-bl cells. Out of 27 viruses, 19 increased their susceptibility to KD-247-mediated neutralization to more than two-fold that of NL/AD8 (19 of 27 clones, 70.4%; Table 1), consistent with previous reports suggesting that the long-term passages *in vitro* select Nab-susceptible HIV-1 [13,14]. Comparing the IC_{50} for each of the mutations, we identified nine NNR mutations that sensitized viruses to KD-247 by more than two-fold (nine of 30 mutations, 30.0%; Table 2). A mutation that altered the IC_{50} no more than two-fold was defined as a non-NNR mutation. Seventeen

Table 1. Summary of half-inhibitory concentration of mutant viruses against KD-247 and b12.

	KD-247		b-12	
Mutations[a]	IC_{50} (μg/m)[b]	Fold sensitization[c]	IC_{50} (μg/m)[b]	Fold sensitization[c]
NL/AD8	357.5 ± 121.8	1	2.4 ± 1.0	1
T48A, D163N, R248M, N297S, S370N, A721T	0.03 ± 0.02	12 342.2	0.2 ± 0.1	12.6
T48A, S186R, S302G S370N, F764S*	7.0 ± 5.5	50.8	0.7 ± 0.2	3.3
S370N, K428E, Q504R, A509T, G689S	39.8 ± 25.9	9.0	1.0 ± 0.3	2.3
D163G, R300G, S370N, S760G	4.4 ± 3.9	82.1	0.4 ± 0.1	6.0
K285R, N298Y, I488T, E506K	480.9 ± 27.1	0.7	1.8 ± 1.1	1.3
E31G, T48A, N279T	141.4 ± 53.1	2.5	1.0 ± 0.2	2.5
D181G, N298Y, S760G	350.0 ± 173.2	1.0	1.8 ± 0.9	1.3
S186R, S370N, S760G	102.8 ± 8.1	3.5	NT	
N298Y, S370N, S760G	380.9 ± 70.7	0.9	1.9 ± 1.0	1.3
V178A, N298Y	89.0 ± 29.3	4.0	8.7 ± 0.9	0.3
N191D, N298Y	157.2 ± 76.8	2.3	1.5 ± 0.9	1.6
I280M, S370N	284.6 ± 34.3	1.3	6.4 ± 0.5	0.4
N297S, S370N	2.4 ± 1.8	149.0	0.8 ± 0.2	3.0
N298Y, E655G*	428.1 ± 47.5	0.8	1.1 ± 0.0	2.3
S370N, N391S	280.5 ± 29.6	1.3	2.5 ± 1.9	1.0
S370N, I546V	303.6 ± 60.8	1.2	2.0 ± 0.2	1.2
S370N, A580T	81.3 ± 18.0	4.4	2.6 ± 0.7	0.9
D163G	6.0 ± 3.5	59.4	1.3 ± 0.0	1.9
D163N	4.8 ± 2.4	74.3	0.9 ± 0.4	2.6
S186R	46.7 ± 24.4	7.7	1.0 ± 0.3	2.4
R248M	59.7 ± 35.8	6.0	2.6 ± 0.7	0.9
N297S	3.0 ± 1.4	119.2	1.2 ± 0.5	2.1
R300G	68.8 ± 28.1	5.2	2.2 ± 1.2	1.1
S302G	6.6 ± 3.4	54.4	2.2 ± 1.1	1.1
S370N	211.5 ± 92.1	1.7	1.2 ± 0.5	2.0
K428E	39.3 ± 35.0	9.1	2.1 ± 0.1	1.2
Q504R	121.6 ± 38.5	2.9	2.7 ± 1.0	0.9

IC_{50}, half-inhibitory concentration; NT, not tested.
[a]NL/AD8 was used as a reference. The amino acid numbering is according to HIV-1AD8 Env. The virus without an asterisk was subjected to virus–antibody binding experiment shown in Fig. 1.
[b]The average and SD from two to 13 independent experiments are shown.
[c]The IC_{50} of the control virus was divided by IC_{50} of each mutant.

Table 2. Summary of mutations characterized in this study.

Mutations[b]	HXB2 coordinate	Location in Env[a]	Fold sensitization
NNR			
D163G	G167	V1/V2	59.4
D163N	G167	V1/V2	74.3
S186R	K192	V1/V2	7.7
R248N	R252	C2	7.0
N297S	N301	V3	119.2
R300G	R304	V3	5.2
S302G	R306	V3	54.4
K428E	K432	C4	9.1
Q504R	Q507	C5	2.9
Non-NNR			
E31G[c]	E32	C1	–
T48A[c]	T49	C1	–
V178A[c]	I181	V1/V2	–
D181G	D185	V1/V2	–
N191D[c]	S195	V1/V2	–
K285R	N289	V3	–
N298Y	N302	V3	–
S370N	S375	C3	–
N391S	X396	V4	–
I488T	I491	C5	–
E506K	E509	C5	–
A509T[c]	A512	gp41	–
I546V	I548	gp41	–
A580T[c]	A582	gp41	–
E655G	E657	gp41	–
G689S[c]	G691	gp41	–
S760G	S762	gp41	–

NNR, nonepitope neutralization regulatory.
[a]The gp120 was subdivided into C1, V1/V2, C3, V3, C4, V4, and C5.
[b]NNR mutations conferring a change in neutralization susceptibility of more than two-fold. Non-NNR mutations are defined as mutations conferring a change in neutralization susceptibility of no more than two-fold.
[c]Estimated from the fold sensitization of a mutant carrying multiple mutations.

non-NNR mutations were also found (Table 2). The magnitude of sensitization by NNR mutations ranged from 2.9 to 119.2. These NNR mutations were present in a broad range of gp120 sites, including V1/V2 loop, C2, V3 loop, C4, and C5. When combined, the NNR mutations additively sensitized the virus to KD-247 by up to 10 000-fold, suggesting an independent structural cross-talk between the V3 loop and each NNR mutation. Such a drastic effect was not observed against b12 Nab targeting the CD4-binding site of gp120 (Table 1). The effect of these NNR mutations appeared to be specific to KD-247, as evidenced by the statistically insignificant correlation between IC_{50} values for KD-247 and b12 (Supplementary Information S1, http://links.lww.com/QAD/A180). This is probably due to the conserved nature of the b12 epitope structure and function. It should be noted that infection with mutant viruses yielded similar levels of luciferase signal from TZM-bl cells when comparable amounts of viruses were used. Also, the viruses bearing six mutations (T48A, D163N, R248M, N297S, S370N, and A721T) replicated in MOLT-4/CCR5 cells with similar efficiency to the no mutation control (NL/AD8), suggesting that replication competency can not account for the change in neutralization susceptibility (data not shown).

Correlation between neutralization susceptibility and KD-247 binding affinity to the virion

We investigated how NNR mutations could sensitize a virus to KD-247-mediated neutralization. We tested whether the KD-247-sensitizing NNR mutation could induce a conformational change in gp120 in such a way that KD-247 became able to bind to gp120 with higher efficiency. To address this question, we performed a capture ELISA in which ELISA plates were precoated with KD-247 and blocked, followed by incubation of virions bearing NNR mutations in the wells of the ELISA plate. The amount of KD-247 captured virus was quantified by ELISA detecting the viral core antigen (Fig. 1). If the latter model is correct, KD-247 captures every mutant with similar efficiencies. As a result, viral binding to KD-247 was significantly correlated with neutralization susceptibility ($P < 0.01$, $n = 26$, two-tailed Student's *t*-test; Fig. 1). These data support a model in which KD-247-sensitizing NNR mutations alter the steady-state structure of gp120 into a conformation such that KD-247 is able to bind to its target with higher efficiencies.

Structural analysis of nonepitope neutralization regulatory mutations

To gain insight into the potential mechanisms whereby KD-247-sensitizing mutations enable neutralization of virions, we used the three-dimensional structural model described by Blay *et al.* [15]. We used an X-ray crystallographic structure with variable loops [15], which was aligned in a trimeric form in accordance with a model developed by Pancera *et al.* [16].

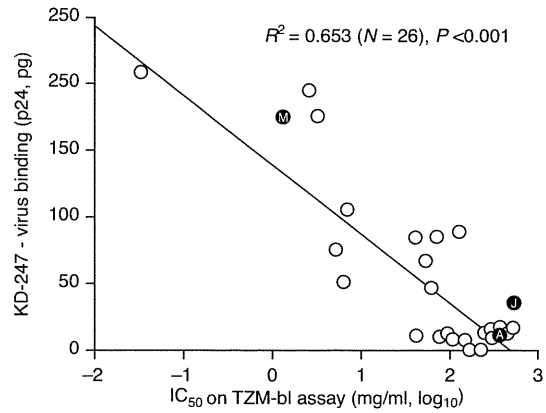

Fig. 1. Analysis of neutralization susceptibility of HIV-1 to KD-247. The half-inhibitory concentration (IC_{50}) for each virus for KD-247 is plotted against the virus capture ELISA data using KD-247 as summarized in Table 1. A significant correlation between the two parameters was detected ($P < 0.01$, two-tailed Student's *t*-test). HIV-1_{MN}, HIV-1_{JR-FL}, and HIV-$1_{NL/AD8}$ are shown as M, J, and A, respectively.

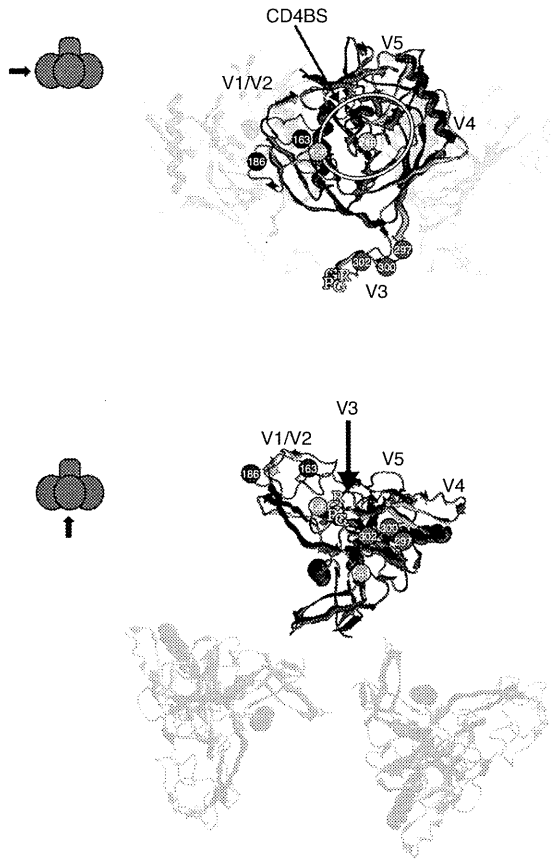

Fig. 2. The three-dimensional mapping of KD-247-sensitizing non-epitope neutralization regulatory mutations based on the Env structure aligned in a trimeric form. The view angle is indicated on the left (arrows) where the gp120 and gp41 are shown in sphere (purple) and rectangle (red), respectively. The gp120 core was shown in blue and red, and the variable loops are shown in yellow. KD-247-sensitizing non-epitope neutralization regulatory (NNR) mutations are indicated by their amino acid numbers. The NNR mutations on the V1/V2 loop, V3 loop, and gp120 core are shown in blue, red, and green, respectively. The GPGR on the V3 loop is shown as a letter code in yellow. The approximate CD4-binding site (CD4BS) is indicated by a white line. The original structural image was developed by Blay *et al.* [15]

The R248N in the C2 region is placed on the gp41 side of the gp120 surface and is not facing the trimeric interface of gp120 (Fig. 2, green) [15]. It has been reported that the H66N, positioned near the trimeric interface of gp120, induces a conformational change of gp120 [17,18]. It has been proposed that H66N alters the quaternary Env structure by acting intermolecularly rather than intramolecularly. In contrast to H66N, the R248N is not positioned at or close to the trimeric surface of gp120. It is likely that R248N induces a different conformational change of the gp120 from H66N, one that does not affect the neutralization susceptibility to b12. It is of interest that the remote KD-247-sensitizing NNR mutation of the gp120 core can specifically affect the conformation of the V3 loop positioned on the gp120 surface.

K428E in the C4 region was mapped in the CD4-binding site close to the so-called bridging sheet (Fig. 2, green), suggesting that the V3 loop and CD4-binding site neutralization epitopes can influence each other's conformation under steady-state conditions. Like R248N, K428E is not positioned at or close to the gp120 trimeric interface. Thus, we speculate that K428E induces a local, not global, Env conformational change. The amino acid corresponding to K428 has been implicated previously in b12 binding through its side-chain as well as through CD4, using HXBc2 Env as a model [19,20]. K428E induces a drastic change in side-chain properties. However, K428E did not significantly affect the viral susceptibility to b12 and the replication efficiency of the NL/AD8 backbone, suggesting that this amino acid may not play a significant role in AD8 Env–b12 interaction. K428 is positioned at the edge of the b12–Env or CD4–Env contact region and, thus, may not contribute significantly to b12–Env or CD4–Env interaction in the context of AD8 Env. Structural cross-talk between the V3 loop and the C4 region under steady-state conditions has been suggested by two studies using monoclonal antibodies. Our approach pinpointed the amino acids responsible for this inter-domain cross-talk.

In contrast to the above two mutations, the precise positioning of KD-247-sensitizing NNR mutations in the V1/V2 and V3 loop is unclear because structural information for them are lacking in the original crystallographic data. According to the molecular dynamics modeling [15], the KD-247-sensitizing NNR mutations in the V1/V2 and V3 loop may not be positioned at or close to the trimeric surface of gp120 (Fig. 2). Instead, they function intramolecularly to affect the conformation of the KD-247 epitope. The Q504R is also lacking in the X-ray crystal structures. However, Q504R is next to the gp120/41 cleavage site and should be close to gp41. The gp41 is relatively proximal to the CD4-binding site of gp120. Some of the mutations in gp41, including T569A and I675V, have been reported to influence the viral susceptibility to Nabs, including b12 [21]. It is conceivable that these mutations in gp41 affect the conformation of gp120. In contrast to T569A and I675V, Q504R is not a b12-sensitizing NNR mutation. Therefore, the conformational change of gp120 induced by Q504R should be distinct from the gp41 mutations.

The structural approach has a potential limitation because the molecular model of Env does not represent the native structure but the liganded structure (Fig. 2). In fact, almost all of the deposited X-ray crystallographic structures are devoid of V1/V2 and/or V3 loops and do not represent the native Env structure, including

the model that our figure is built upon [4,8,15,16,19,22–24].

Discussion

In this work, we identified a number of KD-247-sensitizing NNR mutations using a functional Env library. We re-examined KD-247-sensitive or KD-247-resistant GPGR-positive HIV-1 isolates for NNR mutations and found that KD-247-sensitive viruses, MN (a tissue culture adapted strain of MN) and MNp (a primary HIV-1 isolate), had the mutation equivalent to N301S [25,26]. The predictive value for KD-247 susceptibility due to this mutation was high in the clade B population. However, this does not apply to CRF01_AE, suggesting that this mutation is a clade B-specific predictor of viral susceptibility to KD-247. The other KD-247-sensitizing NNR mutations identified in AD8 did not fully account for the neutralization susceptibility of all of the HIV-1 primary isolates. This suggested that additional NNR mutations should be present, and/or NNR mutations in a given individual virus may function differently than in the other viruses.

How do these mutations alter the conformation of Env to increase the susceptibility of virus to KD-247-mediated neutralization? AD8 is originally resistant to KD-247. One of the molecular mechanisms of AD8 resistance to KD-247 is an epitope-masking by other gp120 domains, possibly the V1/V2 loop or polysaccharides attached to the gp120 [6,27]. Recently, however, Gorny *et al.* [28] reported that the V3 loop of AD8 Env is accessible to KD-247, as AD8 is susceptible to 447–52D-mediated neutralization. This clearly suggests that the sensitization of AD8 strain to KD-247 by the NNR mutations we identified is unlikely due to the removal of the Env domains that physically block antibody access to GPGR epitope. We assume that the V3 loop forms a local conformation in which the neutralization epitope of KD-247 is buried or cannot be recognized by a Nab (local epitope conformation model). When the KD-247-sensitizing NNR mutation occurs, it induces a local, not a global, conformational change of the V3 loop that exposes the neutralization epitope of KD-247. Most of the KD-247-sensitizing NNR mutations are remote from V3 loop. Thus, we assume that KD-247-sensitizing NNR mutations may be located at or close to the interdomain contact regions, and regulate the local conformation of the V3 loop indirectly. Although proven by X-ray crystallographic studies, we propose that the steady-state Env structure is regulated such a way that the domain-independent structural fluctuation is limited. This model predicts that the steady-state structure of the V3 loop is relatively rigid and that its local conformational fluctuation is restricted. This model is relevant to understand the mechanism of action of other NNR mutations against array of Nabs [6–11].

Much attention has been paid to the structural dynamics of HIV-1 Env on CD4 and/or Nab binding. In contrast, not as much attention has been paid to the steady-state conformational dynamics of Env. Unlike previous studies, ours focuses on the steady-state conformational regulation of Env. X-ray crystallography is the best approach to solve a high-resolution native Env structure. However, technical hurdles prevent us from doing so for HIV-1 Env. We examined the mechanism by which the Env conformation is regulated by utilizing Nab KD-247 as a probe. Our approach to identify NNR mutations should complement the crystallization approach in achieving a better understanding of the steady-state structure of HIV-1 Env. Revealing the native structure of Env is critical to the design of an immunogen for the AIDS vaccine and to an understanding of how Env supports virus–cell membrane fusion from the receptor-unbound state.

Acknowledgements

The authors would like to thank Dr Nancy Haigwood for kindly providing the Env structural data. M.T., K.M., E.U., S.K., K.K., S.N., and J.K. designed and performed experiments. T.M., M.H., N.Y., and J.K. analyzed data. J.K. wrote the manuscript.

Conflicts of interest

This work was supported in part by the Japan Health Science Foundation, the Japanese Ministry of Health, Labor and Welfare (H18-AIDS-W-003 and H20-AIDS-G-008 to JK), and the Japanese Ministry of Education, Culture, Sports, Science and Technology (18689014 and 18659136 to J.K.).

There are no conflicts of interest.

References

1. Euler Z, Bunnik EM, Burger JA, Boeser-Nunnink BD, Grijsen ML, Prins JM, *et al.* **Activity of broadly neutralizing antibodies, including PG9, PG16 and VRC01, against recently transmitted subtype B HIV-1 variants from early and late in the epidemic.** *J Virol* 2011; **85**:7236–7245.
2. Hartley O, Klasse PJ, Sattentau QJ, Moore JP. **V3: HIV's switch-hitter.** *AIDS Res Hum Retroviruses* 2005; **21**:171–189.
3. Moore PL, Gray ES, Morris L. **Specificity of the autologous neutralizing antibody response.** *Curr Opin HIV AIDS* 2009; **4**:358–363.
4. Moscoso CG, Sun Y, Poon S, Xing L, Kan E, Martin L, *et al.* **Quaternary structures of HIV Env immunogen exhibit conformational vicissitudes and interface diminution elicited by ligand binding.** *Proc Natl Acad Sci U S A* 2011; **108**:6091–6096.
5. Walker LM, Phogat SK, Chan-Hui PY, Wagner D, Phung P, Goss JL, *et al.* **Broad and potent neutralizing antibodies from an African donor reveal a new HIV-1 vaccine target.** *Science* 2009; **326**:285–289.

6. Walker LM, Burton DR. **Rational antibody-based HIV-1 vaccine design: current approaches and future directions.** *Curr Opin Immunol* 2010; **22**:358–366.
7. Willey S, Aasa-Chapman MM. **Humoral immunity to HIV-1: neutralization and antibody effector functions.** *Trends Microbiol* 2008; **16**:596–604.
8. Zhou T, Georgiev I, Wu X, Yang ZY, Dai K, Finzi A, *et al.* **Structural basis for broad and potent neutralization of HIV-1 by antibody VRC01.** *Science* 2010; **329**:811–817.
9. Wei X, Decker JM, Wang S, Hui H, Kappes JC, Wu X, *et al.* **Antibody neutralization and escape by HIV-1.** *Nature* 2003; **422**:307–312.
10. Gorny MK, Revesz K, Williams C, Volsky B, Louder MK, Anyangwe CA, *et al.* **The v3 loop is accessible on the surface of most human immunodeficiency virus type 1 primary isolates and serves as a neutralization epitope.** *J Virol* 2004; **78**:2394–2404.
11. Gray ES, Moore PL, Bibollet-Ruche F, Li H, Decker JM, Meyers T, *et al.* **4E10-resistant variants in a human immunodeficiency virus type 1 subtype C-infected individual with an antimembrane-proximal external region-neutralizing antibody response.** *J Virol* 2008; **82**:2367–2375.
12. Martin L, Stricher F, Misse D, Sironi F, Pugnière M, Barthe P, *et al.* **Rational design of a CD4 mimic that inhibits HIV-1 entry and exposes cryptic neutralization epitopes.** *Nat Biotechnol* 2003; **21**:71–76.
13. Wrin T, Loh TP, Vennari JC, Schuitemaker H, Nunberg JH. **Adaptation to persistent growth in the H9 cell line renders a primary isolate of human immunodeficiency virus type 1 sensitive to neutralization by vaccine sera.** *J Virol* 1995; **69**:39–48.
14. Zhang YJ, Fredriksson R, McKeating JA, Fenyo EM. **Passage of HIV-1 molecular clones into different cell lines confers differential sensitivity to neutralization.** *Virology* 1997; **238**:254–264.
15. Blay WM, Gnanakaran S, Foley B, Doria-Rose NA, Korber BT, Haigwood NL. **Consistent patterns of change during the divergence of human immunodeficiency virus type 1 envelope from that of the inoculated virus in simian/human immunodeficiency virus-infected macaques.** *J Virol* 2006; **80**:999–1014.
16. Pancera M, Majeed S, Ban YE, Chen L, Huang CC, Kong L, *et al.* **Structure of HIV-1 gp120 with gp41-interactive region reveals layered envelope architecture and basis of conformational mobility.** *Proc Natl Acad Sci U S A* 2010; **107**:1166–1171; Epub 2010 Dec 28..
17. Kassa A, Finzi A, Pancera M, Courter JR, Smith AB 3rd, Sodroski J. **Identification of a human immunodeficiency virus type 1 envelope glycoprotein variant resistant to cold inactivation.** *J Virol* 2009; **83**:4476–4488.
18. Kassa A, Madani N, Schon A, Haim H, Finzi A, Xiang SH, *et al.* **Transitions to and from the CD4-bound conformation are modulated by a single-residue change in the human immunodeficiency virus type 1 gp120 inner domain.** *J Virol* 2009; **83**:8364–8378.
19. Zhou T, Xu L, Dey B, Hessell AJ, Van Ryk D, Xiang SH, *et al.* **Structural definition of a conserved neutralization epitope on HIV-1 gp120.** *Nature* 2007; **445**:732–737.
20. Wu X, Zhou T, O'Dell S, Wyatt RT, Kwong PD, Mascola JR. **Mechanism of human immunodeficiency virus type 1 resistance to monoclonal antibody B12 that effectively targets the site of CD4 attachment.** *J Virol* 2009; **83**:10892–10907.
21. Blish CA, Nguyen MA, Overbaugh J. **Enhancing exposure of HIV-1 neutralization epitopes through mutations in gp41.** *PLoS Med* 2008; **5**:e9.
22. Cho YK, Foley BT, Sung H, Kim YB, Kim JH. **Molecular epidemiologic study of a human immunodeficiency virus 1 outbreak in haemophiliacs B infected through clotting factor 9 after 1990.** *Vox Sang* 2007; **92**:113–120.
23. Huang CC, Tang M, Zhang MY, Majeed S, Montabana E, Stanfield RL, *et al.* **Structure of a V3-containing HIV-1 gp120 core.** *Science* 2005; **310**:1025–1028.
24. Diskin R, Marcovecchio PM, Bjorkman PJ. **Structure of a clade C HIV-1 gp120 bound to CD4 and CD4-induced antibody reveals anti-CD4 polyreactivity.** *Nat Struct Mol Biol* 2010; **17**:608–613.
25. Leavitt M, Park EJ, Sidorov IA, Dimitrov DS, Quinnan GV Jr. **Concordant modulation of neutralization resistance and high infectivity of the primary human immunodeficiency virus type 1 MN strain and definition of a potential gp41 binding site in gp120.** *J Virol* 2003; **77**:560–570.
26. Eda Y, Takizawa M, Murakami T, Maeda H, Kimachi K, Yonemura H, *et al.* **Sequential immunization with V3 peptides from primary human immunodeficiency virus type 1 produces cross-neutralizing antibodies against primary isolates with a matching narrow-neutralization sequence motif.** *J Virol* 2006; **80**:5552–5562.
27. Kwong PD, Wyatt R, Robinson J, Sweet RW, Sodroski J, Hendrickson WA. **Structure of an HIV gp120 envelope glycoprotein in complex with the CD4 receptor and a neutralizing human antibody.** *Nature* 1998; **393**:648–659.
28. Gorny MK, Williams C, Volsky B, Revesz K, Cohen S, Polonis VR, *et al.* **Human monoclonal antibodies specific for conformation-sensitive epitopes of V3 neutralize human immunodeficiency virus type 1 primary isolates from various clades.** *J Virol* 2002; **76**:9035–9045.

AIDS RESEARCH AND HUMAN RETROVIRUSES
Volume 27, Number 00, 2011

DOI: 10.1089/aid.2011.0180

The Hematopoietic Cell-Specific Rho GTPase Inhibitor ARHGDIB/D4GDI Limits HIV Type 1 Replication

Tadashi Watanabe,[1] Emiko Urano,[2] Kosuke Miyauchi,[2] Reiko Ichikawa,[2] Makiko Hamatake,[2] Naoko Misawa,[1] Kei Sato,[1] Hirotaka Ebina,[1] Yoshio Koyanagi,[1] Jun Komano[2]

Abstract

Rho GTPases are able to influence the replication of human immunodeficiency virus type 1 (HIV-1). However, little is known about the regulation of HIV-1 replication by guanine nucleotide dissociation inhibitors (GDIs), one of the three major regulators of the Rho GTPase activation cycle. From a T cell-based cDNA library screening, ARHGDIB/RhoGDIβ, a hematopoietic lineage-specific GDI family protein, was identified as a negative regulator of HIV-1 replication. Up-regulation of ARHGDIB attenuated the replication of HIV-1 in multiple T cell lines. The results showed that (1) a significant portion of RhoA and Rac1, but not Cdc42, exists in the GTP-bound active form under steady-state conditions, (2) ectopic ARHGDIB expression reduced the F-actin content and the active forms of both RhoA and Rac1, and (3) HIV-1 infection was attenuated by either ectopic expression of ARHGDIB or inhibition of the RhoA signal cascade at the HIV-1 Env-dependent early phase of the viral life cycle. This is in good agreement with the previous finding that RhoA and Rac1 promote HIV-1 entry by increasing the efficiency of receptor clustering and virus-cell membrane fusion. In conclusion, the ARHGDIB is a lymphoid-specific intrinsic negative regulator of HIV-1 replication that acts by simultaneously inhibiting RhoA and Rac1 functions.

Introduction

The human immunodeficiency virus type I (HIV-1) is the causative agent of acquired immunodeficiency syndrome (AIDS). The clinical success of Maraviroc, an antiretroviral drug that targets the host cell protein CCR5, demonstrates the importance of understanding host-HIV-1 interaction as this information will provide the basis for the development of the next generation of antiretroviral drugs. HIV-1 replicates primarily in CD4-positive T cells. However, aside from the viral receptors CD4 and CCR5, few lymphoid cell-specific regulators of HIV-1 replication have been identified. This is partly due to the use of nonlymphoid cells to screen for cellular factors that regulate HIV-1 replication, as these cells support the efficient transduction of genetic materials. Therefore, T cell-based cDNA library screening has some advantages, as discussed later.

Members of the Rho GTPase family, including RhoA, Rac1, and Cdc42, have been reported to regulate the replication of HIV-1 at various stages of the viral life cycle, including viral entry, transcription, and viral release.[1–7] Although these proteins are widely expressed, genome-wide screens for proteins that regulate HIV-1 replication using siRNA or shRNA libraries have failed to identify Rho GTPases.[8–10] This may suggest that Rho GTPases are not potent regulators of HIV-1 replication and are therefore difficult to detect unless the viral replication assay is employed, since multiple replication cycles augment the biological effects of Rho GTPases.

There are three major regulators of the activation cycle of Rho GTPases: guanine nucleotide exchange factors (GEFs), GTPase-activating proteins (GAPs), and guanine nucleotide dissociation inhibitors (GDIs or ARHGDIs). RhoGEFs promote the exchange of GDP for GTP, RhoGAPs accelerate GTP hydrolysis, and ARHGDIs stabilize the GDI-bound form of Rho GTPases and also mask the lipid moiety of Rho GTPases, thereby sequestering Rho GTPases at the plasma membrane.[11–14] Some RhoGAPs and RhoGEFs have been known to regulate HIV-1 replication.[6,9,10,15–18] Positive regulators of Rho GTPases, such as RhoGEFs, were identified in the genome-wide screens, although these studies yielded varying results. In this sense, the upstream regulators of Rho GTPases may more potently influence HIV-1 replication than Rho GTPases themselves when expression levels are dysregulated. ARHGDIs have yet to be identified as regulators of HIV-1 replication.

[1]Laboratory of Viral Pathogenesis, Institute for Virus Research, Kyoto University, Kyoto, Japan.
[2]AIDS Research Center, National Institute of Infectious Diseases, Tokyo, Japan.

Previously, we established a genetic screening system using a T cell-derived cDNA library to isolate cellular factors that render cells resistant to HIV-1 replication.[19,20] This system is unique in that the screen is based on MT-4 cells, a human CD4-positive T cell line, which were exposed to replication-competent HIV-1. Using this system, the carboxy-terminal domains of Brd4 and SEC14L1a were found to be negative regulators of HIV-1 replication.[19,20] Importantly, these factors were not found in previous genetic screens, suggesting that our system complements other genome-wide analyses. In this study, we describe a lymphoid-specific RhoGDI that negatively regulates HIV-1 replication through attenuation of both RhoA and Rac1 functions.

Materials and Methods

Cells

Cells were maintained in RPMI 1640 medium (Sigma, St. Louis, MO) supplemented with 10% fetal bovine serum (FBS; Japan Bioserum, Tokyo, Japan or Thermo Fisher Scientific Inc., Waltham, MA), 50–100 U/ml penicillin, and 50–100 μg/ml streptomycin (Invitrogen, Tokyo, Japan), and then incubated at 37°C in a humidified 5% CO_2 atmosphere. The selection of cDNA library-transduced cells was described previously.[20] To select puromycin-resistant cells after infection with pQc- or pSM2c-based murine leukemia virus (MLV) vector, 1 μg/ml puromycin (Sigma) was added to the culture medium.

Plasmids

The plasmid vectors pCMMP, pMDgag-pol, pSV-tat, phRL/CMV, and pVSV-G were described previously.[21] The shRNA expression vectors pSM2c and pSM2/ARHGDIB (RHS1764-9680880) were purchased from Thermo Fisher Scientific (Open Biosystems Products, Huntsville, AL). The pQcXIP was obtained from Clontech (BD Biosciences Clontech, Palo Alto, CA). pGEX-Rhotekin-RBD and pGEX-4T-PAK2-RBD were kindly provided by S. Narumiya, Kyoto University.[3,22] To construct pLTR-hRL, the HIV-1_{HXB2} long terminal repeat (LTR) was amplified by PCR using the following primers: 5′-GGA TCC TGG AAG GGC TAA TTC ACT CC-3′ and 5′-GCT AGC TGC AGC TGC TAG AGA TTT TCC ACA CTG-3′. The *BglII-NheI* fragment of the PCR product was cloned into the corresponding restriction sites of phRL/CMV, generating pLTR-hRL. The LTR-Luc plasmid was described previously.[23] To construct pCMV-Tat-FLAG, HIV-1_{NL4-3} *tat* was amplified from cDNA prepared from HIV-1-infected MT-4 cells by RT-PCR using the following primers: 5′-ATG GAG CCA GTA GAT CCT AGA CTA GAG CCC T-3′ and 5′-TTC CTT CGG GCC TGT CGG GT-3′. The PCR product was cloned into the *EcoRV* sites of pcDNA3.1 Zeo(+) bearing FLAG-tags at the *NotI-XhoI* site (Invitrogen). The pCMV-Luc plasmid was a generous gift from Dr. Hijikata (Kyoto University).

Flow cytometry

Cells were incubated with anti-CD4, anti-CD8, or anti-CXCR4 monoclonal antibodies conjugated to R-phycoerythrin (PE; BD Pharmingen, San Diego, CA) for 30 min at 4°C. Cells were washed once with phosphate-buffered saline (PBS) supplemented with 1% FBS and analyzed by FACS Calibur (Beckton Dickinson, San Jose, CA).

Phalloidin staining of F-actin

Phalloidin staining of F-actin was performed as described previously.[24] In brief, cells were fixed, permeabilized by cytofix/cytoperm (BD Bioscience) for 20 min on ice, washed, and stained with Alexa Fluor 647-phalloidin (Invitrogen) for 30 min at 4°C. Samples were kept on ice until analysis by FACS Calibur or Canto II (Beckton Dickinson, San Jose, CA). The flow cytometric data were analyzed using FlowJo version 9.3 (Tree-star Inc., Ashland, OR).

Viruses

The retroviral vector pCMMP, carrying the MT-4 cDNA library and a green fluorescent protein (GFP) expression cassette, was obtained from Takara (Takara, Otsu, Japan). Full-length ARHGDIB was cloned from a lymph node cDNA library (Takara) by RT-PCR using the primers 5′-GCA CCG GTC TCG AGC CAC CAT GAC TGA AAA AGC CCC AGA GC-3′ and 5′-CCA ATT GGA TCC TCA TTC TGT CCA CTC CTT CTT AAT CG-3′, and cloned into the pCMMP vector. The MLV vectors were produced by tripartite transfection of pMDgag-pol, pVSV-G, and either pCMMP, pQc, or pSM2c retroviral vector. Cells were infected with the MLV vectors as described previously.[21] The production of replication-competent HIV-1_{HXB2} and the measurement of replication kinetics were performed as described previously.[21]

Western blotting

Western blotting was performed according to techniques described previously.[25] The following monoclonal antibodies were used: anti-RhoA (C-11; Santa Cruz Biotechnology, Santa Cruz, CA), anti-Rac1 (23A8; Millipore, Japan), anti-Cdc42 (B-8; Santa Cruz Biotechnology), anti-ARHGDIB (A01; Abnoba, Taiwan), anti-$p24^{CA}$ (183-H12-5C; NIH AIDS Research and Reference Reagent Program), anti-actin (clone C4; Millipore), and anti-tubulin (DM1A; Sigma). Densitometric analysis was performed using ImageJ ver. 1.43 software (obtained from http://rsbweb.nih.gov/ij/index.html).

Active Rho GTPase capture assay

We adopted a protocol described previously.[3,22] In brief, the glutathione *S*-transferase (GST) fused to the Rho GTPase binding domain (RBD) of Rhotekin and GST fused to the RBD of PAK2 were expressed in *E. coli* and purified by incubating the cell lysates with glutathione-Sepharose 4B beads (GE Healthcare Bio-Sciences, Piscataway, NJ) for 3 h at 4°C. The beads were washed three times with ice-cold Rho buffer (25 mM HEPES, pH 7.5, 150 mM NaCl, 10 mM $MgCl_2$, 1 mM EDTA, 10% Glycerol). Finally, the beads were washed with ice-cold Rho buffer supplemented with 1% NP-40 and protease inhibitor cocktail tablets (Complete, Roche Diagnostics GmbH, Mannheim, Germany). Cells were incubated in ice-cold Rho buffer for 15 min on ice, and the cell lysates were clarified by centrifugation at 18,000 × *g* at 4°C for 20 min. A fraction of the cleared cell lysates was incubated at 37°C for 30 min as a negative control or coincubated with GTPγS (0.1 mM, Sigma) for 30 min at 30°C as a positive control. These preparations were incubated with the above beads at 4°C for 1 h. The beads were washed three times with Rho buffer containing 1% NP-40 and subjected to SDS-PAGE followed by Western blotting. The bead-bound GTPases were detected

using a monoclonal antibody against RhoA, Rac1, or Cdc42, as appropriate.

Single-round infection assay

Single-round virus infection and luciferase assays were performed as described previously.[21,26] In brief, cells were exposed to viral preparations containing 1–10 ng of $p24^{CA}$. Luciferase activities were measured at 2–3 days postinfection with the Picagene luciferase assay kit (Toyo Ink, Tokyo, Japan) or Steady-Glo kit (Promega, Tokyo, Japan) according to the manufacturer's protocols. For the inhibition of Rho-kinase (ROCK), cells were pretreated with 12.5 μM Y27632 (Nakalai tesque, Kyoto, Japan) for 1 h and incubated with the viral preparation in the presence of 12.5 μM Y27632 for 4 h. Cells were washed with tissue culture medium and cultivated for 2 days. Light emission was detected with a 1420 ARVOSX multilabel counter (Perkin Elmer, Wellesley, MA) or a Veritas luminometer (Promega).

Single-round production assay

Five million PM1/control or PM1/ARHGDIB cells were resuspended in 250 μl of STBS (25 mM Tris-Cl, pH 7.4, 137 mM NaCl, 5 mM KCl, 0.6 mM Na_2HPO_4, 0.7 mM $CaCl_2$, and 0.5 mM $MgCl_2$), including 10 μg of pHXB2 proviral plasmid DNA. Cells were mixed with 250 μl of STBS containing 1 mg/ml of DEAE-Dextran and incubated for 30 min at room temperature (RT). The cells were then incubated with STBS containing 10% DMSO for 2 min at RT and washed with 1 ml HBSS (Invitrogen). Transfected cells were cultured in RPMI medium containing 10% FBS and 1 μM efavirenz. After 2 days in culture, viruses in the culture supernatant were pelleted by ultracentrifugation on a 20% sucrose cushion. Cells and viruses were lysed with radioimmunoprecipitation assay (RIPA) lysis buffer (0.05 M Tris-HCl, 0.15 M NaCl, 1% Triton X-100, 0.1% sodium dodecyl sulfate, and 1% sodium deoxycholate) and electrophoresed in a 10% polyacrylamide gel for SDS–PAGE. Proteins were then transferred to a PVDF membrane, and $p24^{CA}$ was detected by immunoblot analysis using an anti-$p24^{CA}$ antibody.

Reporter expression assay

The luciferase-expressing reporter plasmids were transfected into PM1 cells according to the DEAE-Dextran method as described above. For transfection, either 1 μg of pCMV-Luc, 10 μg of pLTR-Luc, 0.5 μg of phRL/CMV, or 1 μg of pLTR-hRL was used. The pLTR-Luc and pLTR-hRL were co-transfected with 5 μg of pCMV-tat-FLAG and 1 μg of pSVtat, respectively. Firefly luciferase activity was measured as described above. Renilla luciferase activity was also measured as described above, except that the Renilla Luciferase Assay System (Promega) was used in place of the Steady-Glo kit. The data were analyzed using a two-tailed Student's *t*-test.

Results

Identification of RhoGDIβ/ARHGDIB as a negative regulator of HIV-1 replication

A pool of MT-4 cells constitutively expressing a cDNA library transduced with an MLV-based retroviral vector was used to screen for possible regulators of HIV-1 replication. The MLV vector carried an expression cassette for GFP and inserts from a cDNA library derived from MT-4 cells (Fig. 1A). The cDNA-transduced cells were enriched with a cell sorter using GFP as a marker. These cells were then infected with CXCR4-using (X4) $HIV\text{-}1_{HXB2}$. MT-4 cells have been shown to support efficient HIV-1 production and rapidly undergo cell death after infection. The surviving MT-4 cells were propagated and genomic DNA was isolated to identify the inserted cDNA, as described previously.[19] These genes were considered potential negative regulators of HIV-1 replication. A cDNA clone encoding ARHGDIB (RhoGDIβ/LyGDI/D4GDI; gene ID 397) was recovered from the MT-4 cDNA library (1/94 independent clones, 1.1%).

Full-length ARHGDIB cDNA was cloned into the MLV vector pQcXIP, and a T cell line expressing ARHGDIB at levels higher than endogenous levels was established. To verify the HIV-1-resistant phenotype of ARHGDIB, the rate of HIV-1 replication was assessed in MT-4 cells subjected to ectopic ARHGDIB expression. In these cells, ARHGDIB levels were increased by approximately 4.9-fold compared with control cells, while the cell surface expression of CD4 and CXCR4 was not significantly affected in MT-4 cells (Fig. 1B). Even the modest up-regulation of ARHGDIB delayed HIV-1 replication kinetics (Fig. 1B). Suppression of HIV-1 replication was independently reproduced in MT-4 cells, even when a different retroviral vector, pCMMP, was used to transduce ARHGDIB (data not shown). In addition, neither the rate of cell proliferation nor cell morphology was affected by stable ectopic expression of ARHGDIB over at least 6 months in culture (data not shown). Delayed HIV-1 replication in cells ectopically overexpressing ARHGDIB was also observed in PM1 (Fig. 1C), M8166 (Fig. 1D), and Jurkat cells (Fig. 1E), in which ARHGDIB levels were increased by 2.1-, 1.9-, and 1.5-fold, respectively, compared with control levels. Similar data were also obtained in SUP-T1 cells (data not shown). The delayed HIV-1 replication in cells ectopically expressing ARHGDIB was reproduced in 10 independent experiments ($p < 0.01$, two-sided binomial test), strongly suggesting that ARHGDIB attenuates the replication of HIV-1. These results indicate that enhanced expression of ARHGDIB renders cells resistant to HIV-1 replication. Consistent with these data, the shRNA-mediated down-regulation of ARHGDIB accelerated the replication of HIV-1 in MT-4 cells (Fig. 1F). These data support the idea that ARHGDIB is a negative regulator of HIV-1 replication.

The RhoGDI family has three members, α, β, and γ, which correspond to ARHGDI A, B, and C, respectively.[11] RhoGDI family members are known to regulate Rho GTPases, including RhoA, Rac1, and Cdc42, although some nonredundant functions of RhoGDIs have been reported.[27] ARHGDIB/RhoGDIβ is primarily expressed in cells of a hematopoietic lineage. Given that Rho GTPases are known to be positive regulators of HIV-1 replication and that ARHGDIB is a negative regulator of Rho GTPases in hematopoietic cells, the function of ARHGDIB was investigated in further detail.

Molecular mediators in the inhibition of HIV-1 replication by ARHGDIB

Under *in vitro* culture conditions, T cell lines show a constitutively activated cell phenotype, and Rho GTPases, including RhoA, Rac1, and Cdc42, have been implicated in T cell

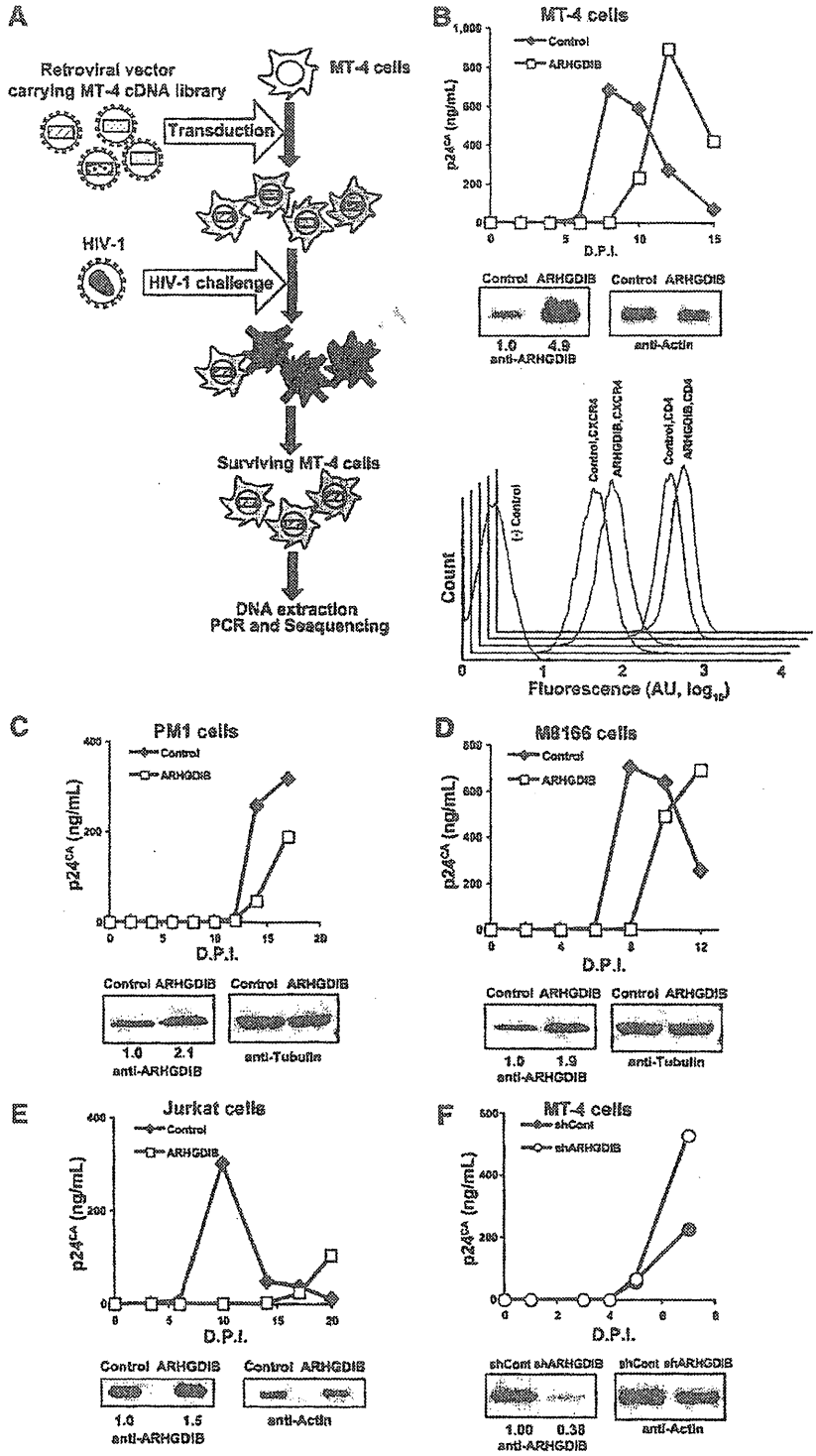

FIG. 1. Isolation and characterization of ARHGDIB as a negative regulator of HIV-1 replication. (A) The screening strategy used to isolate genes that render MT-4 cells resistant to HIV-1 replication. (B–E) Ectopic expression of ARHGDIB (open rectangles) in MT-4 (B), PM1 (C), M8166 (D), and Jurkat (E) cells delayed the replication kinetics of HIV-1. Representative data from five, two, and two independent experiments for MT-4, M8166, and Jurkat cells are shown, respectively. The control counterpart is shown as filled diamonds. (B) The flow cytometric profiles of MT-4 cell surface CD4 and CXCR4 are shown. MT-4/ARHGDIB cells stained for CD8 were used as a negative control. (F) Down-regulation of ARHGDIB (open circles) in MT-4 cells accelerated the replication of HIV-1. The control counterpart is shown as filled circles. (B–F) Expression levels of ARHGDIB and an internal control, either actin or tubulin, were assessed by Western blot analysis. The magnitude of ARHGDIB up- or down-regulation was determined by densitometry and is indicated below each image. AU, arbitrary unit; D.P.I., days postinfection.

activation.[28–30] These Rho GTPases are expressed in various T cell lines, including MT-4, PM1, and M8166 cells, as confirmed by RT-PCR analysis (data not shown). It seemed likely that augmented ARHGDIB expression affected HIV-1 replication by modulating the activity of these Rho GTPases. Thus, the activation status of RhoA, Rac1, and Cdc42 was determined in relation to the enhanced expression of ARHGDIB.

Rho GTPases are intrinsically inefficient hydrolyzing enzymes that quickly cycle between GTP-bound active and GDP-bound inactive forms. If ARHGDIB attenuates HIV-1 replication by inhibiting Rho GTPase activities, some fraction of Rho GTPases would exist in a GTP-bound active form under steady-state tissue culture conditions, and this population should be decreased in cells ectopically expressing ARHGDIB. Using an active Rho GTPase capture assay, the levels of active Rho GTPases in control and ARHGDIB-expressing cells were measured (Fig. 2A). In this assay, GTP-bound Rho GTPase is captured by glutathione-Sepharose beads conjugated to GST fused to the Rho binding domain of Rhotekin or PAK2. The active forms of both RhoA and Rac1, but very little Cdc42, were detected in PM1 cells under steady-state tissue culture conditions (Fig. 2B–D). Activation levels under the steady-state conditions were estimated by comparing the captured Rho GTPase signals with the maximal activation levels, which were established by converting all Rho GTPases to an active form by GTPγS before the pull-down procedure. The activated fractions of Rac1, RhoA, and Cdc42 were 34.2%, 23.2%, and 0.0%, respectively (Fig. 2B–D). Importantly, ectopic expression of ARHGDIB reduced the activated fractions of RhoA and Rac1 to 4.1% and 3.6%, respectively (Fig. 2B and C). Similar observations were made for MT-4 and SUP-T1 cells (data not shown).

These observations clearly indicated that ARHGDIB attenuates RhoA and Rac1 activity simultaneously in these T cell lines and suggested that RhoA and Rac1 are the primary targets of ectopically expressed ARHGDIB. Note that RhoA and Rac1 levels were increased by 1.4- and 1.3-fold, respectively, in cells ectopically expressing ARHGDIB, according to the densitometric analysis (Fig. 2B and C). This is due to the ARHGDIB-mediated stabilization of Rho GTPases, as

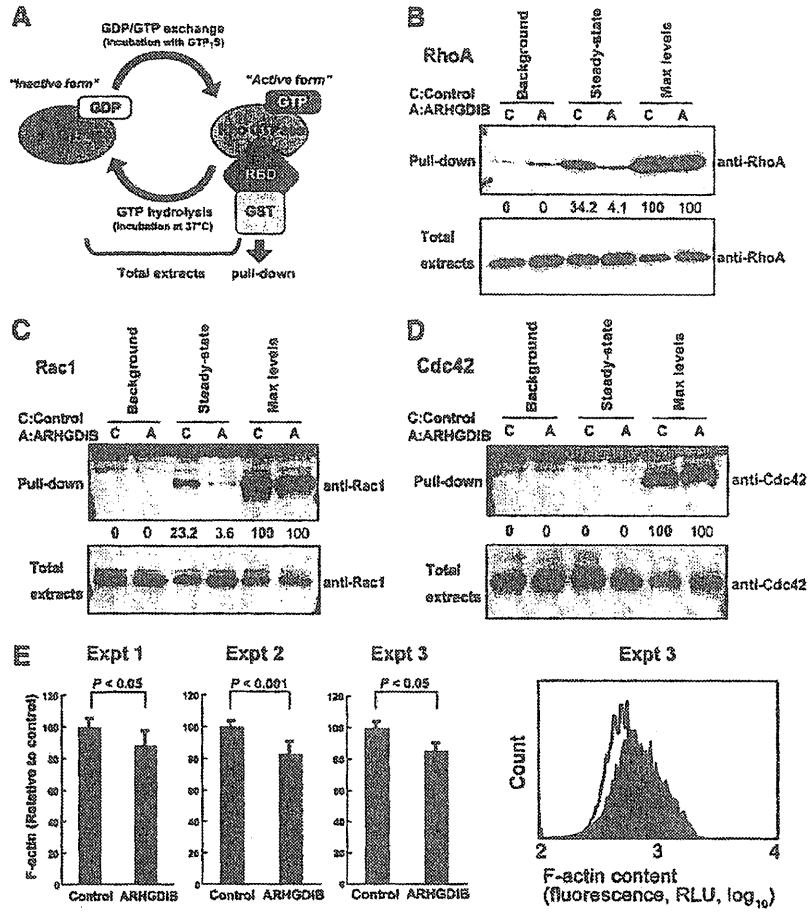

FIG. 2. Activation of RhoA and Rac1 under steady-state conditions in PM1 cells. (A) The experimental procedure for the active Rho GTPase capture assay. The active GTP-bound form is collected by glutathione-Sepharose beads coated with an RBD-GST fusion protein and compared with the total expression levels of each Rho GTPase by Western blot analysis. Incubation of the cell lysate with GTPγS shifts the equilibrium to the right, and incubation of the cell lysate at 37°C for 30 min shifts it to the left, representing the maximal activation levels (Max levels in B–D) or the background levels (background in B–D) of each Rho GTPase, respectively. (B–D) Activation of RhoA (B), Rac1 (C), and Cdc42 (D) in PM1 cells. The activation levels under steady-state conditions were estimated by densitometric analysis defined by setting the Max levels and background to 100% and 0%, respectively. (E) Measurement of F-actin content in PM1/ARHGDIB and control cells. Data from three independent experiments are shown in the bar graphs, and each of these experiments was performed in triplicate. The right panel shows the flow cytometric profile of Experiment 3, in which PM1/ARHGDIB is indicated by a black line, and the control is shown in gray. Statistical significance between the two groups was analyzed by two-tailed Student's *t*-test. AU, arbitrary unit.

reported previously.[31] This effect is modest in Cdc42 (1.1-fold, Fig. 2D) because the capture of Rho GTPase by ARHGDIB depends on the active GDP/GTP exchange cycle of Rho GTPase under steady-state conditions, which occurs inefficiently in Cdc42.

The common effector function of RhoA and Rac1 is the reorganization of the actin cytoskeleton.[11,12,32,33] If the ectopic expression of ARHGDIB inhibits RhoA and Rac1 effector function, the monomer-polymer actin equilibrium in ARHGDIB-transduced cells should be shifted toward a depolymerized state.[13,14,34] To test this, flow cytometry using fluorescently labeled phalloidin, which binds to F-actin, was used to measure the amount of polymerized actin. Under steady-state conditions, the fluorescence intensity of PM1/ARHGDIB cells was significantly lower than in control cells (Fig. 2E). The reduction levels of F-actin content in PM1/ARHGDIB cells were 14.2±1.6% ($N=3$, $p<0.05$ by Student's *t*-test, two-tailed; Fig. 2E) compared with the control. A similar trend was observed in SUP-T1 cells. These data are in agreement with the results obtained by the active Rho GTPase capture assay and the previous findings that the overexpression of RhoGDI in various cell lines induces the disruption of actin cytoskeleton-dependent processes.[35–37] These data indicate that the ectopic expression of ARHGDIB in T cells suppresses the activation status of both RhoA and Rac1 under steady-state tissue culture conditions.

Analysis of the viral life cycle in ARHGDIB-expressing T cells

Next, the mechanism by which ARHGDIB blocks HIV-1 replication was investigated. To do this, the viral entry and production phases were examined separately.

To examine the viral entry phase, PM1/ARHGDIB cells were infected with X4-tropic HIV-1_{NL4-3} Env- or VSV-G-pseudotyped HIV-1 that produces luciferase upon the establishment of infection. In these viruses, luciferase is under the regulation of a long terminal repeat (LTR) or cytomegalovirus (CMV) promoter. When the relative luciferase activity in the control cells was set at 100%, the infection efficiency of HIV-1 Env-pseudotyped HIV-1 expressing luciferase driven by the HIV-1 LTR promoter was 33.0±2.6% ($N=3$, $p<0.001$ by Student's *t*-test, two-tailed; Fig. 3A). Similar results were observed in MT-4 cells (data not shown). In contrast, the infection efficiency of VSV-G-pseudotyped HIV-1 expressing luciferase with either the HIV-1 LTR or CMV promoter was 243.2±31.9% ($N=3$, $p<0.01$; Fig. 3A) or 480.3±158.1% ($N=3$, $p<0.05$; Fig. 3A), respectively. Similarly, infection with VSV-G-pseudotyped MLV driving the expression of luciferase with the MLV LTR promoter was 10.0±6.4-fold more efficient in PM1/ARHGDIB than in control cells ($N=4$, $p<0.05$; Fig. 3A). To examine the effect of ARHGDIB on gene expression, reporter plasmids driving the expression of luciferase with either the CMV or HIV-1 LTR promoter were transfected into PM1 cells. The LTR- and CMV-driven luciferase activities in PM1/ARHGDIB cells were modestly increased compared with the control cells, but not decreased (2.1±0.6-fold, and 2.4±1.6-fold for LTR- and CMV-driven constructs, six and four independent experiments, respectively; Fig. 3B). Taken together, these data suggest that the inhibition of viral entry is specific to HIV-1 Env, and the early phase of the viral life cycle is strongly affected.

When measured by flow cytometry, PM1/ARHGDIB cells were found to express cell surface CD4 at levels 1.4-fold higher than control cells (average of four independent experiments), while the cell surface levels of CXCR4 were 0.8-fold higher (average of five independent experiments). Considering that ARHGDIB did not affect the levels of cell surface CD4 or CXCR4 in MT-4 cells (Fig. 1B) and M8166 cells (data not shown), and that the reduction in CXCR4 expression in PM1 cells is relatively modest, these data suggest that changes in the expression of viral receptors do not fully account per se for the decreased susceptibility of PM1/ARHGDIB cells to HIV-1_{NL4-3} Env-pseudotyped HIV-1.

To examine the production phase, proviral DNA was transfected into PM1/ARHGDIB and the control cells, and the viral protein expression in cells and the level of viral production in the culture supernatant were measured. The transfected cells were cultured in the presence of the antiretroviral drug efavirenz, which inhibits the replication cycle of HIV-1, allowing the assessment of viral production in the transfected cells. The levels of viral Gag in PM1/ARHGDIB cells, which are cleaved by protease to yield multiple bands in Western blot analysis with an anti-$p24^{CA}$ antibody, were comparable to the control cells (Fig. 3C). To assess these data quantitatively, densitometric analysis was conducted to quantify the signals representing $Pr55^{Gag}$, MA-CA, and $p24^{CA}$. Then, the percentage of $p24^{CA}$ and MA-CA relative to the total signal was calculated; this represented the efficiency of Gag processing. The Gag processing efficiency was 75.5% in PM1/ARHGDIB cells, similar to the control cells (69.9%). In addition, the ratio of the total signal in the viral lysate to that in the cell lysate was calculated. This reflects the efficiency of viral production. The virus/cell intensity ratios were 0.43 and 0.56 for the controls and cells ectopically expressing ARHGDIB, respectively. Similar data were obtained in an independent experiment in PM1 cells. These data suggest that the negative effect of ARHGDIB on the viral production phase was undetectable in T cells.

A single-round HIV-1 infection experiment was performed in the presence of a specific ROCK inhibitor, Y27632, to test whether the effector functions of RhoA are critical in regulating HIV-1 infection. The inhibition of ROCK, a RhoA signal mediator, reduced HIV-1 infection by 48.6±6.3% compared with the control levels ($N=4$, $p<0.05$ by Student's *t*-test, two-tailed; Fig. 3D). These observations suggested that the RhoA signal triggered by HIV-1 Env-receptor interaction is involved in the regulation of HIV-1 infection. This inhibition of ROCK accounted for approximately 77% of the inhibition of HIV-1 infection in PM1 cells ectopically expressing ARHGDIB (33.0% vs. 48.6%; Fig. 3A and D). These data also suggested that Rac1 plays a supplementary role in the restriction of HIV-1 infection. Taken together, this suggests that ARHGDIB limits HIV-1 replication primarily by affecting Env-mediated processes, most likely via receptor clustering and virus-cell membrane fusion.

Discussion

A handful of lymphoid-specific cellular regulators of HIV-1 replication are known, including CD4 and CCR5. However, few hematopoietic lineage-specific inhibitors of HIV-1 replication have been identified. Recently a dendritic- and myeloid-cell-specific restriction factor SAMHD1 has been

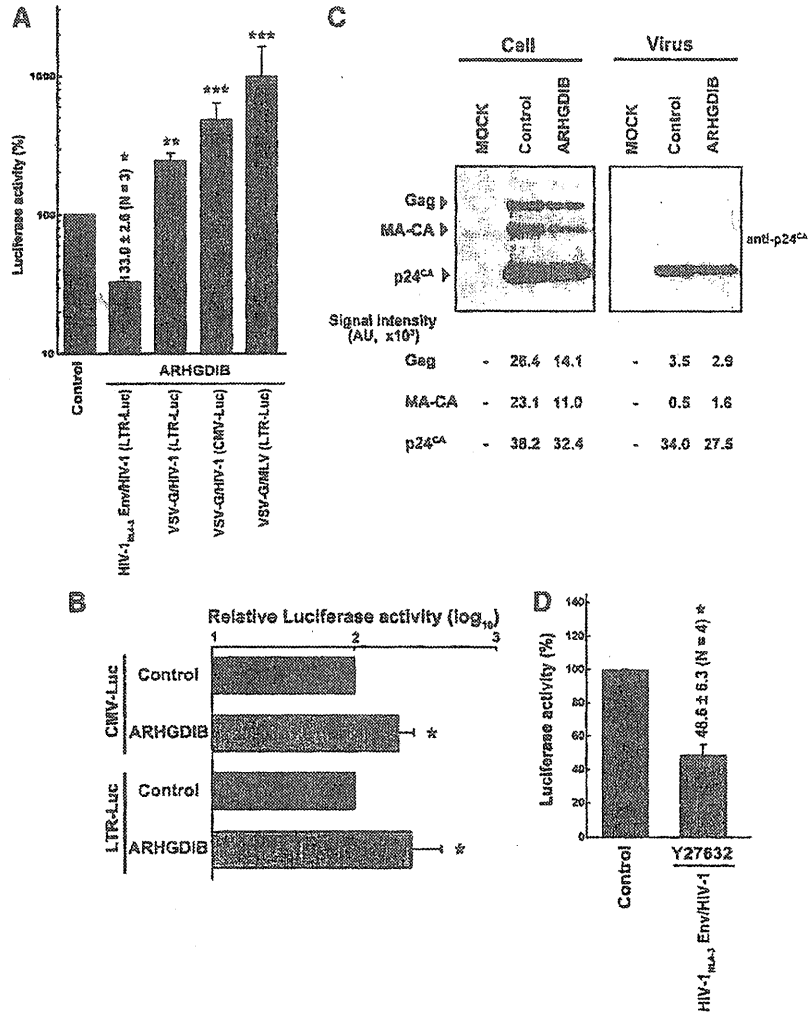

FIG. 3. The effect of ARHGDIB expression on the HIV-1 life cycle. (A) Single-round infection assay using replication-incompetent HIV-1 and MLV expressing luciferase upon integration, pseudotyped either with HIV-1 Env or with VSV-G. The promoters driving the expression of luciferase are noted in parentheses. Luciferase signals detected in PM1/ARHGDIB cells (gray) relative to control cells (black) are shown. The data represent the average and standard deviation from three or four independent experiments. Statistical significance between each group and the control was analyzed by two-tailed Student's *t*-test (single asterisk, $p < 0.001$; double asterisk, $p < 0.01$; and triple asterisk, $p < 0.05$). (B) Transient transfection assay to assess the effect of ARHGDIB on reporter gene expression. CMV- or HIV-1 LTR-driven luciferase expression vectors were introduced into PM1/control or PM1/ARHGDIB cells. Luciferase signals detected in PM1/ARHGDIB cells (gray) relative to control cells (black) are shown. The average and standard deviation from four and six independent experiments for CMV and LTR constructs, respectively, are shown. Statistical significance between PM1/ARHGDIB and the control was analyzed by two-tailed Student's *t*-test (asterisk, $p < 0.05$). (C) Viral production was assessed by transfecting proviral DNA into PM1/ARHGDIB and control cells. Viral protein levels in the cell lysate (Cell) and the pellet from the culture supernatant (Virus) were measured by Western blot analysis using anti-$p24^{CA}$ monoclonal antibody. The expression levels of Gag, MA-CA and $p24^{CA}$ were assessed by densitometric analysis and are shown in the lower panel. (D) Single-round infection assay in the presence of a ROCK inhibitor, Y27632. Luciferase signals detected in PM1/ARHGDIB cells (gray) relative to control cells (black) are shown. The data represent the average and standard deviation from four independent experiments. Statistical significance between each group and the control was analyzed by two-tailed Student's *t*-test (asterisk, $p < 0.05$).

reported.[38] APOBEC3 family members, which exhibit antiretroviral activity, may be hematopoietic cell specific, although their expression levels in non-T cells have not been directly examined.[39,40] In this study, we showed that modest up-regulation of the hematopoietic cell-specific RhoGDI, ARHGDIB, negatively regulated HIV-1 replication in various T cell lines, while it appeared to have no impact on cell proliferation. ARHGDIB is a constitutively expressed, lymphoid-specific protein. Therefore, ARHGDIB could provide intrinsic immunity against HIV-1 infection. In contrast, APOBEC3 family members are primarily interferon inducible.

RhoGDIs have not been isolated as negative regulators of HIV-1 replication in previous genetic screening studies. This is partly because nonlymphoid cells were used to screen genetic materials and the siRNA/shRNA-based gene knockdown is not able to identify negative regulators of HIV-1 replication at high sensitivity. Moreover, previous screens could not identify all potential factors, especially those present in the hematopoietic cell lineage, since nonlymphoid cells were often used. Our T cell-based screen using replication-competent HIV-1 allowed us to identify ARHGDIB as an HIV-1 inhibitor.

Rho GTPases play multiple roles in cell biology, including actin reorganization, endocytosis, and tubulin regulation, and ARHGDIB is a negative regulator of Rho GTPases.[11–14,32,41,42] It has been reported previously that inhibition of RhoA affects